

ZIBELINE INTERNATIONAL  
PUBLISHING

ISSN: 2521-0920 (Print)

ISSN: 2521-0602 (Online)

CODEN: MJGAAN

## Malaysian Journal of Geosciences (MJG)

DOI: <http://doi.org/10.26480/mjg.02.2023.154.172>

## RESEARCH ARTICLE

## HYDROCARBON EXPLORATION AND RESOURCE OPTIMIZATION THROUGH SEQUENCE STRATIGRAPHIC ANALYSIS AND DATA AUGMENTATION OF HIGH FIELD OFFSHORE WESTERN NIGER DELTA

Adebayo Sunday Samuel<sup>a</sup>, Osisanya Olajuwon Wasiu<sup>b</sup>, Ighrakpata C. Fidelia<sup>c</sup>, Ibitoye Taiwo Abel<sup>d</sup>, Fagbemigun, Tokunbo Sanmi<sup>e</sup><sup>a</sup>Department of Applied Geophysics, Federal University of Technology Akure, Ondo State, Nigeria.<sup>b</sup>Department of Physics, University of Benin, Benin City, Edo state, Nigeria<sup>c</sup>Department of Physics, College of Education, Edjeba, Warri South, Delta State.<sup>d</sup>Department of Petroleum Engineering and Geosciences, Petroleum Training Institute, Effurun, Nigeria.<sup>e</sup>Department of Geophysics, Federal University, Oye-Ekiti, Nigeria.\*Corresponding Author Email: [wasiu.osisanya@uniben.edu](mailto:wasiu.osisanya@uniben.edu)

This is an open access journal distributed under the Creative Commons Attribution License CC BY 4.0, which permits unrestricted use, distribution, and reproduction in any medium, provided the original work is properly cited

## ARTICLE DETAILS

## Article History:

Received 18 November 2023

Revised 20 December 2023

Accepted 09 January 2024

Available online 11 January 2024

## ABSTRACT

Efficient hydrocarbon exploration and resource optimization are vital for sustainable oil reservoir development. This necessitates a profound grasp of source rocks and trapping systems, typically gleaned from subsurface seismic studies followed by drilling for resource extraction. Additionally, interpreting stratigraphic data is critical for identifying productive reservoirs, distinguishing low-yield from high-yield sands, and reducing exploration risks and costs. Our study aims to enhance subsurface structure and stratigraphic understanding, specifically identifying potential hydrocarbon reservoirs, source rock formations, sealing structures, stratigraphic traps, and depositional environments. In the Niger Delta region, we seek to reduce operational costs and exploration risks related to oil and gas exploration. In the "high field" offshore Niger Delta, our research combines well logs and seismic data to define hydrocarbon trapping potential, stratigraphic profiles, and depositional settings. The stratigraphic sequence is systematically divided into system tracts by five sequence boundaries, maximum flooding surfaces, and transgressive surfaces that reveal different depositional environments. This integrated approach pinpoints two prospective areas, P1 and P2, as potential hydrocarbon reservoirs. The analysis of seismic data and well logs is highly effective in identifying subsurface structures conducive to hydrocarbon accumulation within the stratigraphic framework. Furthermore, the alternation of lowstand, transgressive, and highstand system tracts suggests favorable conditions for source rocks, sealing formations, and reservoirs, improving the prospects for successful hydrocarbon exploration and resource optimization.

## KEYWORDS

Well logs, Hydrocarbon accumulation, Depositional Environment, System tracts

## 1. INTRODUCTION

Sequence stratigraphy is a useful tool for better understanding subsurface stratigraphy by delineating the source rocks, seals, and reservoirs. Not all the wells drilled in the Niger Delta are successful. This may be due to a lack of detailed understanding of the stratigraphic and structural settings. Hooper et al. (2002) state that a contractional zone defined by a fold-thrust belt developed in a toe-of-slope setting is connected to regional and counter-regional growth faults that were developed in an outer-shelf and upper-slope setting through a translational zone that contains shale diapirs. To effectively demarcate the structures that are conducive to hydrocarbon accumulation, a thorough understanding of subsurface configurations is required (Coffen 1984). The reason behind this is that hydrocarbons are present in geologic traps, which are any arrangements of rock formations that prevent gas and oil from escaping in a vertical or lateral direction. But there are two types of these traps: stratigraphic and structural. Seismic data and well logs together would significantly improve the degree of reliability in mapping complex structural and stratigraphic plays (Adejobi and Olayinka 1997; Barde et al. 2000, 2002). From parallel to sub-parallel to chaotic, its internal reflection geometries go through this range. According to Ayuk et al. (2022) seismic structural maps provided

impressions of rock deformation and hydrocarbon potential in relation to the field. The study intends to offer a thorough understanding of the geological features and suggest data enhancements for more precise interpretations and decision-making in order to lay a strong foundation for future hydrocarbon exploration and exploitation in the study area. It specializes in the fields of geology and petroleum exploration, specifically focusing on sequence stratigraphy and its implications for hydrocarbon exploration. Here's a breakdown of the key elements of the scope of the research:

- Sequence Stratigraphy Analysis: Sequence boundaries, maximum flooding surfaces, and transgressive surfaces are examples of important geological features that have been identified by the study using sequence stratigraphy. Understanding the geological past and the possibility of hydrocarbon reservoirs depends on these characteristics.
- Cyclic Patterns: The research area's cyclical pattern of alternating tracts of the Lowstand (LST), Transgressive (TST), and Highstand (HST) systems suggests that there may be hydrocarbon source rocks present. This pattern also suggests that the conditions are favorable for the generation and accumulation of organic matter.
- Reservoir Potential: The study suggests that reservoir quality sands are

## Quick Response Code



## Access this article online

## Website:

[www.myjgeosc.com](http://www.myjgeosc.com)

## DOI:

10.26480/mjg.02.2023.154.172

present within the LST and HST, indicating the potential for hydrocarbon reservoirs.

- iv. **New Prospects:** The research has identified two new prospects (P1 and P2) with coordinates and existing producing reservoirs (HIGH1, HIGH2, HIGH3, and HIGH4) that can potentially increase hydrocarbon reserves. Thereby providing guidance on how to improve future exploration efforts and enhance the understanding of the geological environment.

**1.1 Regional Geology of Niger Delta**

The Niger Delta clastic wedge originated along a failed arm of an aulacogen triple junction system, which first formed in the late Jurassic during the breakup of the South American and African plates (Burk 1972; Whiteman 1982). While the third failed arm created the Benue Trough, the two arms that followed the coasts of Cameroon and Nigeria's southwest and southeast eventually became West Africa's passive continental margin. Buildups in the delta were also caused by other depocenters along the African Atlantic coast. Synrift sediments accumulated from the Cretaceous to the Tertiary, with the Albian age representing the oldest dated sediments. There were several transgressive and regressive phases in the deposition of the thickest successions of synrift marine and marginal marine clastics and carbonates (Doust and Omatsola 1989). Basin inversion during the Santonian (late Cretaceous) period marked the end of the synrift phase. The Benue Trough was crossed by the sea, causing further subsidence as the continents split apart. The Middle Cretaceous saw the Niger Delta clastic wedge continue to prograde into a depocentre above the collapsed continental margin at the triple junction. The Benue and Bida Basins, two failed rift arms, were the primary drainage systems that supplied sediment. During the Late Cretaceous, there were periodic transgressions that stopped the sediment from progressing. Sediment was primarily supplied during the Tertiary from the north and east via the Niger, Benue, and Cross Rivers. Significant volumes of volcanic debris from the Cameroon volcanic zone, which began in the Miocene, were supplied by the Benue and Cross Rivers. As these drainage areas evolved and basement subsidence persisted, the Niger Delta clastic wedge prograded into the Gulf of Guinea at a rate that increased steadily. With more sediment having accumulated since the Oligocene, regression rates rose during the Eocene (Ilevbare1, 2020; Omorogieva)

Tertiary Niger Delta deposits have been found to exhibit three major depositional cycles (Doust and Omatsola 1989; Short and Stauble 1967). The first two involved a major marine transgression in the Paleocene and started with a marine incursion during the middle Cretaceous, primarily

involving marine deposition. The second of these two cycles, which begins in the late Paleocene and ends in the Eocene, shows how a "true" delta with an arcuate coastline dominated by waves and tides is developing. The age of these sediments spans from the Quaternary in the south to the Eocene in the north. The deposits belonging to the most recent depositional cycle have been separated by significant synsedimentary fault zones into six depobelts, also referred to as mega sequences or depocenters.

These depobelts developed as a result of sediment accumulation concentrated in specific areas of the delta due to structural deformation patterns limiting sediment supply pathways. As local accommodations were filled and the locus of deposition shifted basinward, these depobelts changed positions over time (Doust and Omatsola, 1989). These depobelts align sub-parallel to the current shoreline, striking northwest-southeast (Figure 1). From the Eocene in the north to the Pliocene offshore of the current shoreline, depobelts get progressively younger as one moves basinward (Doust and Omatsola, 1989). The delta edge, central delta, and distal delta are identified as the three main regions. From an early stage spanning the Paleocene to an early Eocene to a later stage of delta development in the Miocene, the morphology of the Niger Delta changed (Figure 2). Early coastlines were concave toward the sea, and basement topography had a significant impact on deposit distribution (Doust and Omatsola, 1989). There were two main axes of delta progradation. The first ran parallel to the Niger River and was caused by a sediment supply that was greater than the rate of subsidence. Smaller in size than the first, it became active in the basinward direction of the Cross River during the Eocene to early Oligocene, when shorelines advanced into the Olumbe-1 area (Short and Stauble, 1967). The Ihuo Embayment divided this axis of deposition from the main Niger Delta deposits, and later advancing deposits of the Cross River and other nearby rivers rapidly filled it in (Short and Stauble, 1967). When these distinct eastern and western depocentres merged in the early to middle Miocene, late stages of deposition started. The delta prograded sufficiently into the basin during the late Miocene that shorelines became broadly concave. This swift delta progradation's accelerated loading moved the unstable shales underneath. The strata above were deformed by these shales as they rose into diapiric walls and swells. Major erosion events occurred along the leading progradational edge of the Niger Delta as a result of the complex deformation structures that followed, causing local uplift. Many deep canyons that are filled with clay today are thought to have formed during periods of low sea level. These canyons are carved out of the shelf. According to Reijers et al. (1997) and Tuttle et al. (1999), the most well-known are the Afam, Opuama, and Qua Iboe Canyon fills.

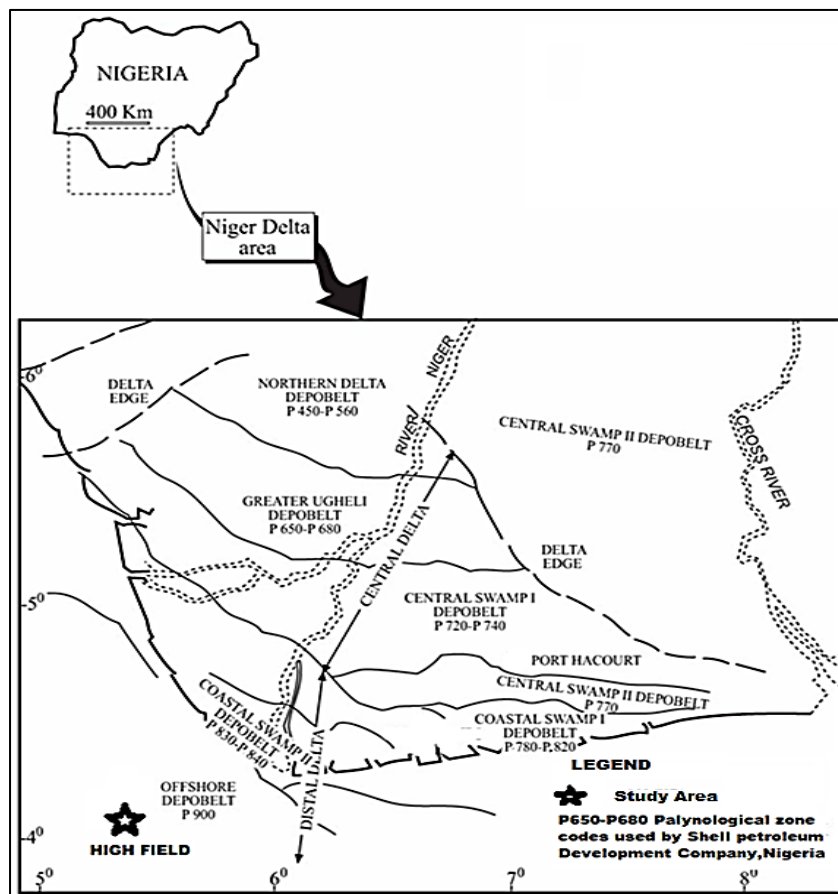


Figure 1: Depobelts with their relative ages striking northwest-southeast, (After Doust and Omatsola 1989).

| AGE         | FORMATION | LITHOLOGY              | THICKNESS  | SEDIMENTARY CYCLE | ENVIRONMENT            |
|-------------|-----------|------------------------|------------|-------------------|------------------------|
| Holocene    | BENIN     | [Lithology: Sandstone] | max 2100m  | DELTA             | CONTINENTAL            |
| Pleistocene |           |                        |            |                   |                        |
| Pliocene    |           |                        |            |                   |                        |
| Miocene     | AGBADA    | [Lithology: Sandstone] | 3000m      | REGRESSION        | TRANSITIONAL TO MARINE |
| Oligocene   |           |                        |            |                   |                        |
| Eocene      | AKATA     | [Lithology: Shale]     | 600-16000m | TRANSGRESSION     | MARINE                 |
| Paleocene   |           |                        |            |                   |                        |

Figure 2: Generalized lithostratigraphy of Niger Delta (Nwangwu, 1990).

1.2 Niger Delta Stratigraphy

Short and Stauble (1967) describe the stratigraphic evolution of the Cretaceous strata beneath and the Tertiary Niger Delta provide descriptions of the petroleum geology of the Niger Delta (Tuttle et al., 1999; Doust and Omatsola, 1989; Evamy et al., 1978). Using sequence stratigraphic methods, (Stacher, 1995) created a hydrocarbon habitat model for the Niger Delta. The physiography, sedimentation, and depositional environments of the contemporary Niger Delta were characterized by (Allen, 1965; Oomkens, 1974). The Niger Delta's three main lithostratigraphic units the Akata, Agbada, and Benin Formations

(Figure 3) regress in age basinward, which is indicative of the clastic wedge's overall depositional environment's regression. In southern Nigeria, there are exposed stratigraphic equivalent units to these three formations.

Stratigraphic traps are probably just as significant as structural traps on the delta's flanks (Beka and Oti, 1995). Sandstone pockets can be found in this area in between diapiric structures. This alternating sequence of sandstone and shale gradually grades to essentially sandstone towards the delta toe (base of the distal slope).

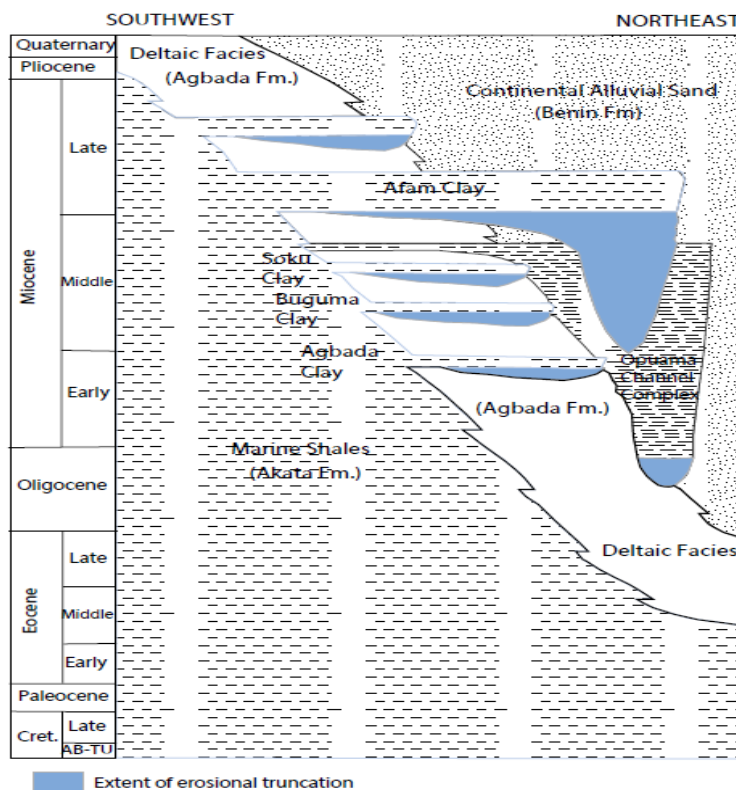


Figure 3: Stratigraphic column showing the three formations of the Niger Delta. (Shannon and Naylor, 1989; Doust and Omatsola, 1989).

1.3 Petroleum Generation and Migration

The top of the current oil window in the Niger Delta was determined by Evamy et al. (1978) to be at the 240°F (115° C) isotherm. The upper Akata Formation and lower Agbada Formation contain the oil window, or active source-rock interval, in the northwest section of the delta. The top of the

oil window is stratigraphically lower to the southeast (Evamy et al., 1978). The top of the oil window's distribution is attributed by some researchers (Nwachukwu and Chukwura, 1986; Doust and Omatsola, 1989; Stacher, 1995) to the thickness and sand/shale ratios of the overburden rock (Benin Formation and variable proportions of the Agbada Formation).



## 1.4 Concept of Seismic Sequence Stratigraphy

Sedimentary basin fills are divided into genetic packages by sequence stratigraphy, which is defined by the unconformities and their corresponding conformities (Emery and Myers 1996). For stratigraphic prediction and the correlation and mapping of sedimentary facies, it serves as a chronostratigraphic framework. The sequence stratigraphic approach incorporates elements of sedimentology, biostratigraphy, chronostratigraphy, and seismic stratigraphy, among other geological disciplines (Posamentier and James, 1993). Sequence stratigraphy has proven to be a crucial tool in seismic and well-log interpretation, as it aids in the prediction of traps, the analysis of basin evolution, and the spatial distribution of reservoir and source rocks. Sequence stratigraphy has been defined of genetically related strata within the context of surfaces that are important for chronostratigraphy (Posamentier et al., 1988; Van Wagoner, 1995).

## 2. METHODOLOGY

In order to identify system tracts within each depositional sequence and seismic facies and to delineate potential reservoirs, source rocks, seals, stratigraphic traps, and depositional environments within the study area, stratigraphic interpretation was performed using well logs and 3-D seismic data. The lateral distributions of the identified facies were carried out using Root Mean Square (RMS) Amplitude Attribute Analysis.

### 2.1 Lithostratigraphic Well Correlation

Lithostratigraphic well correlation of sand bodies within the Agbada Formation was carried out along the West-East direction using resistivity log and gamma ray log to determine the lithologies penetrated by the studied wells. This was done as a prelude to the determination of the top and base of the Agbada Formation using the reflection characteristics of the 3-D seismic volume, stratigraphic indicators, and the nature of the gamma ray curves that characterize the interval. For the gamma ray logs, 65 API was chosen as the cut-off point.

## 3. DISCUSSION OF RESULTS

### 3.1 Lithostratigraphic Well Log Correlation

Gamma ray and resistivity logs were used to correlate the lithostratigraphic well logs (Figure 4a-b). There are seven sand bodies that have been identified: Sand A, B, C, D, E, G, and F. The recognized sand bodies still contain intercalations of shales but are not clean. Sand A is the thickest, with a range of 4600 feet (1402.1 meters) to 7400 feet (2255.5 meters), while Sand B is the deepest, with a range of 7500 feet (2286.0 meters) to 7900 feet (2407.9 meters). Sand C, D, E, F, and G span a distance of 8060 feet (2456.7 meters) to 8900 feet (2712.7 meters), 9100 feet (2773.7 meters) to 9400 feet (2865.1 meters), 9500 feet (2895.6 meters) to 10300 feet (3139.4 meters), 10500 feet (3200.4 meters) to 10850 feet (3307.08 meters), and 11100 feet (3383.28 meters) to 11250 feet (3429 meters), in that order. Because hydrocarbons have high resistivities if they are not biodegraded, sands E, F, and G are likely hydrocarbon reservoirs based on the resistivity log. The lithology found in the logged intervals is primarily composed of sand and shale that alternate at a ratio of roughly 65:35.

### 3.2 Interpretation of Sequence Boundaries (SBs), Maximum Flooding Surface (MFSs) and Systems Tracts

The results are shown in Figs. 5a and 5b and discussed below, after Sequence Boundaries (SBs), Maximum Flooding Surfaces (MFSs), and Systems Tracts have been identified.

#### 3.2.1 Sequence Boundaries (SBs)

Seismic and well log data were used to identify the five Sequence Boundaries (SB<sub>1</sub>, SB<sub>2</sub>, SB<sub>3</sub>, SB<sub>4</sub>, and SB<sub>5</sub>). SBs were identified as an erosional surface between a lowstand and a highstand system tract based on the interpretation of well logs. They were found to be situated between two maximum flooding surfaces (Figure 5a-b). Every log signature clearly identifies SB<sub>1</sub>, and every field well has penetrated it. The location of the wells on the block and in relation to one another affect the depth of occurrence.

This boundary is associated with a blocky log signature. It is connected to a graded sandy shale sequence boundary. The non-uniform log shape suggests that the lithology was deposited in a high- to moderate-energy regime with little time for sediment sorting, which led to the intercalation of the beds and subsequent aggradations. This is a feature of a channel complex environment that acts as an appropriate and distinct demarcation for the lowstand system tract that lies on top of it. Except for SB<sub>2</sub>, other Sequence Boundaries have a comparable log motif. They exhibit

a channel sand deposit that is abruptly marked by a complex of slope wedge deposits, and they resemble the blocky log shape seen in the log motif. Unlike other patterns that aggrading uniformly, SB<sub>2</sub> began with a progradational (not very noticeable) pattern.

#### 3.2.2 Maximum Flooding Surfaces (MFSs)

On the well logs, five maximum flooding surfaces were selected. These surfaces indicate locations where a thick layer of shale starved of terrigenous material occurs. The point where the surfaces occur is shown by the resistivity curve's lowest value, which equates to the gamma ray curve's highest value.

#### 3.2.3 Interpretation of System Tracts

In this study, system tracts comprising lowstand, transgressive, and highstand were identified. Every system tract exhibited a distinct signature on well logs and was deposited at a consistent location within an interpreted base level cycle brought on by eustasy.

#### 3.2.4 Lowstand Systems Tract (LST)

A sequence boundary forms the base of the Lowstand Systems Tract (LST), which is made up of the oldest deposits within a depositional sequence. Slope fans, prograding wedge complexes, and basin floor fans make up this system. The basin floor complex, shown in Figure 5a-b, was identified at HIGH 2. Typically, this massive sand body contains sand of exceptional quality, well at the depth intervals 10823 - 10641 ft (3299-3243 m), and 7861 - 7685 ft (2396-2342 m), at HIGH 1 well at the depth of 11022-10871 ft (3360-3313 m) and 7888 - 7649 ft (2404-2331 m), at HIGH 4 well at the depth 10844-10619 ft (3305-3237 m), 9406-9325 ft (2867-2842 m), 7877-7698 ft (2401-2346 m) and 6812 - 6612 ft (2076-2015 m), at HIGH 3 well at depth 10799-10612 ft (3292-3235 m), 7946-7750 ft (2421-2362 m). In the same vein, according to Umar et al., 2020. Because of the primary reservoir's high porosity (24%), maximum reservoir thickness (0.9), and low AI (8 106 kg/m<sup>2</sup>s), it can produce the highest possible gas yield. An overall coarsening upward pattern, which is interpreted as a gradual overall shallowing upward pattern from marine to non-marine environments, characterizes the prograding complex, the uppermost unit of the LST. Only shoreline areas along the outer shelf experience sand deposition; these areas include shoreface and fluvial facies, which typically exhibit an upward well log pattern that coarsens (Mitchum et al., 1993). In HIGH 2, the prograding complex is found at the depth of 10614-10500 ft (3243-3200 m), 9322-9082 ft (2841-2768 m) and 6813 - 6351 ft (2077-1925 m), HIGH 1 at the depth intervals 10871 - 10889 ft (3313-3322 m), 9305 - 9088 ft (2836-2770 m), 7649 - 7500 ft (2331-2286 m), and 6386 - 6360 ft (1946-1938 m), in HIGH 4 at the depth intervals 10619 - 10524 ft (3236-3208 m) and 9325 - 9140 ft (2842-2786 m); and in HIGH 3 at the depth interval 9740 - 9375 ft (2869-2858 m) and 7750-7550 ft (2362-2301 m), (Figure 5b).

#### Transgressive Systems Tract (TST)

An ideal depositional sequence has this as its middle systems tract. As sea levels rise more quickly, the transgressive systems tract (TST) forms (Mitchum et al., 1993). All the wells under study exhibited its recognition, which is typified by retrogradational parasequence sets (Figure 5a-b). In HIGH 2, it was found at the depth intervals 11631 - 11213 ft (3545-3418 m), 11115 - 10823 ft (3388-3299 m), 10495-10205 ft (3199-3110 m), 9082-8890 ft (2768-2710 m), 7496-7429 ft (2285-2264 m) and 6351 - 6308 ft (1936-1922 m); in HIGH 1 at the depth intervals 11593 - 11423 ft (3534-3482 m), 11312 - 11072 ft (3448-3375 m), 10888-10316 ft (3319-3144 m), 9088-8908 ft (2770-2715 m), 7491-7119 ft (2283-2170 m) and 6357-6250 ft (1937-1905 m) and in HIGH 4 at the depth interval 11507-11188 ft (3507-3410 m), 11120-10844 ft (3389-3305 m), 10524 - 10237 ft (3208-3120 m), 9143-8942 ft (2787-2726 m), 7508 - 7376 ft (2288-2248 m) and 6360-6299 ft (1939-1920 m); and in HIGH 3 at the depth interval 11655-11500 ft (3552-3505 m), 11128-10799 ft (3392-3292 m), 10612-10491 ft (3235-3198 m), 9376 - 9138 ft (2968-2785 m) and 7550-7416 ft (2301-2260 m).

#### Highstand Systems Tract (HST)

According to Mitchum et al. (1993), the top unit of a depositional sequence is represented by the highstand systems tract (HST). Early gradational to later pro-gradational parasequence sets define it. In HIGH 2, HST occurs at the depth intervals 11213- 11125 ft (3418-3391 m), 10205 - 9322 ft (3110-2841 m), 7429- 6822 ft (2283-2079 m) and 6308 - 5500 ft (1922-1674 m); in HIGH 1, at the depth interval 11422 - 11384 ft (3481-3470 m), 10316-9307 ft (3144-2837 m), 8880-7877 ft (2707-2401 m), 7419-6838 ft (2261-2084 m) and 6297-5500 ft (1919-1676 m) and in HIGH 4, at the depth interval 11426- 11188 ft (3483-3410 m), 10237-9406 ft (3120-2867 m), 8942-7877 ft (2726-2401 m), 7376-6812 ft (2248-2076

m) and 6309-5471ft (1923-1668 m); and in HIGH 3 at the depth interval 11500-11128 ft (3505-3392 m), 10457-9750 ft (3187-2972 m), 9133-7946 ft (2784-2422 m) and 7416-6837 ft (2260-2084 m) (Figure 5a-b).

**3.2.5 Depositional Sequences Stratigraphic Interpretation**

The Type-1 depositional sequences found in the wells under study include LST, which are composed of prograding complexes, TST, and HST, and basin floor fan. Seismic sections and wells both identify four distinct depositional sequences; however, wells are only utilized in the comprehensive interpretation of depositional sequences.

**Depositional Sequence 1**

This depositional sequence starts at depth 11022 ft (3360 m) and ends at 9327 ft (2843 m) for HIGH 1 well, 10823 ft - 9322 ft (3299-2841 m) for HIGH 2, 11844 ft - 9406 ft (3610-2867 m) for HIGH 4 and 10799 - 9740 ft (3292-2969 m) for HIGH 3 well. Beginning this sequence, the lowstand system tract is delimited below by a sequence boundary (SB1). Above the boundary, the sand package is characterized as a prograding complex with an upward coarsening trend capped by a small condensed section linked to an abundance and diversity peak that ends at the maximum shale point (transgressive surface, TS). This is comprised of an overall retrograding parasequence stacking pattern capped by maximum flooding surface MFS2, and is overlaid by the transgressive system tract (TST) above the TS1 (Figure 5a-b). The TST is where the highstand system tract rests. It begins with a stacking pattern of aggradation parasequences and then begins to prograde upward. It is terminated by another sequence boundary, SB<sub>2</sub>, at the top.

**Depositional Sequence 2**

This depositional sequence occur at a depth of 9322 -7869 ft (2841-2398 m), 9327 -7888 ft (2842-2404 m), 9406 -7877 ft (2867-2401 m) and 9740 -7946 ft (2969-2422 m) for HIGH 2, HIGH 1, HIGH 4 and HIGH 3 wells respectively. This sequence is started by the Lowstand system tract. Sequence boundary SB<sub>2</sub> (Figure 5a-b) forms the base boundary for the entire sequence. This system tract's sediment package exhibits the rounded log signature of an aggradational Prograding complex. For the HIGH 2 well, the Transgressive System Tract crosses the LST and descends

to a depth of 8890 feet. It is distinguished from the major condensed section of the shelf environment by the laterally extensive shale blanket (TS3), which is made up of a maximum flooding surface (MFS3) and a series of fining upward retrograding parasequence patterns (Figure 5a-b). At a depth of 7869 feet to 7946 feet for the four wells immediately below depositional sequence 2, the highstand system tract caps depositional sequence 2. This system tract shows aggradational parasequence pattern as it progrades upward with shales interval above to be capped by another sequence boundary SB<sub>3</sub>.

**Depositional Sequence 3**

The lower sequence boundary of this depositional Sequence 3 occurs at 7869 ft (2398 m), 7888 ft (2404 m), 7877 ft (2401 m), and 7946 ft (2421 m) for HIGH 2, HIGH 1, HIGH 4 and HIGH 3 wells respectively while the top of the sequence occurs at 6818 ft (2078 m), 6836 ft (2084 m), 6812 ft (2076 m) and 6837 ft (2084 m) for HIGH 2, HIGH 1, HIGH 4 and HIGH 3 wells respectively, with prograding complex pattern as it is overlain by the transgressive system tract. At a depth of 7677 feet (2340 meters) for the HIGH 4 well, the maximum flooding surface with the lowest shale resistivity value and high value on the gamma ray log can be found (Figure 5 a-b). The highstand system tract coarsening upward pattern, which is immediately above the marker surface, is covered in blocky aggradational prograded sand.

**Depositional Sequence 4**

All of the wells exhibit this depositional sequence, with the exception of HIGH 3, where it is entirely absent. This could be because of historical erosion processes. Depositional Sequence 3 observed in the study area is bounded at the base and top by sequence boundaries at depths 6818 ft (2078 m), 6836 ft (2084 m), 7877 ft (2401 m), and 5496 ft (1675 m), 5500 ft (1676 m), 5488 ft (1673 m) for HIGH 2, HIGH 1, and HIGH 3 wells respectively. It starts with a lowstand systems tract, overlain by a transgressive system tract that is truncated by a maximum flooding surface MFS<sub>5</sub>. The Highstand System Tract, which reaches from the top of the maximum flooding surface to a depth of 7877 feet (2401 meters) and denotes the top of the sequence for the HIGH 3 well, caps this sequence (Figure 5a-b).

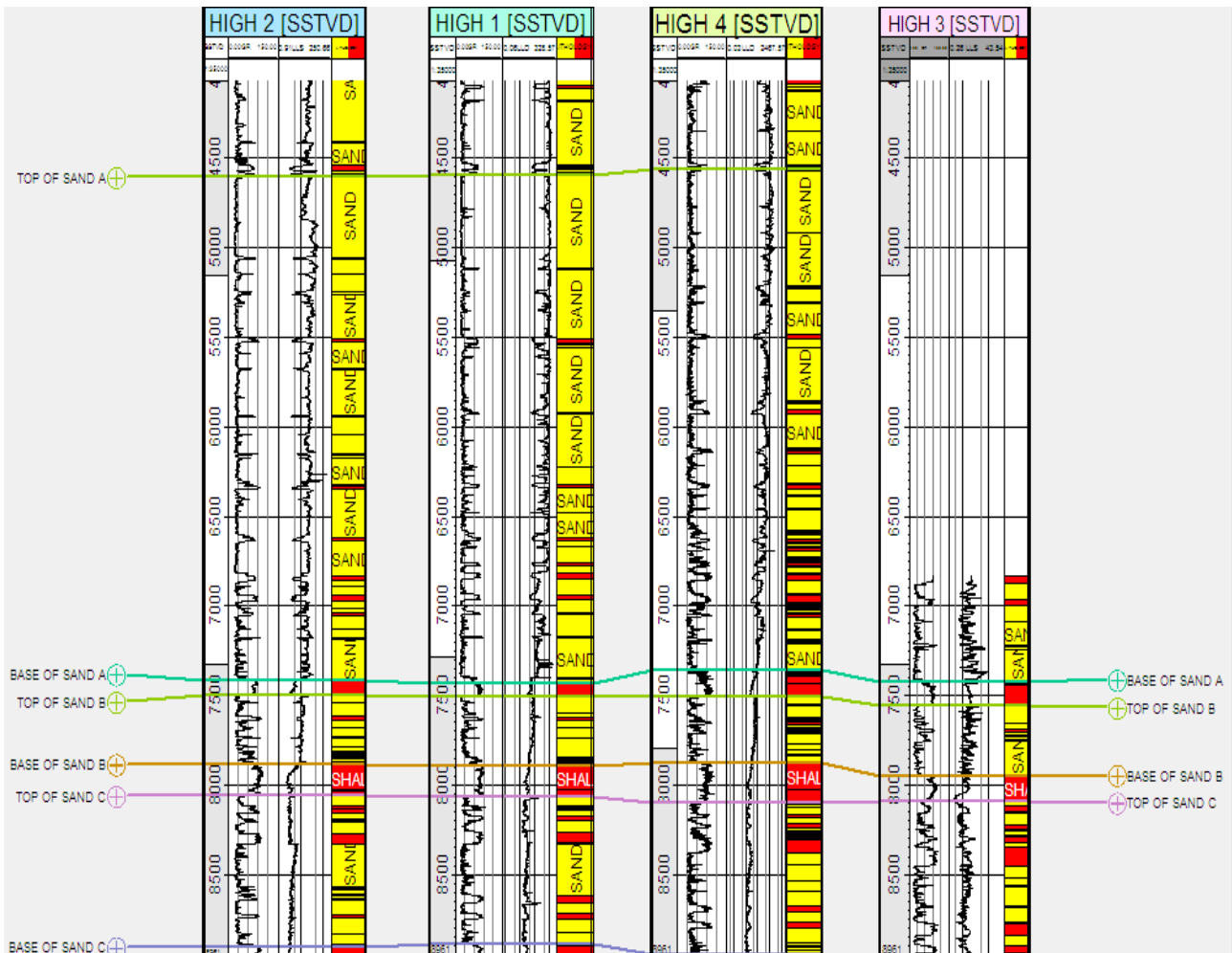


**Figure 4a:** Lithostratigraphic Well Correlation of Sand A to Sand B along West-East direction.

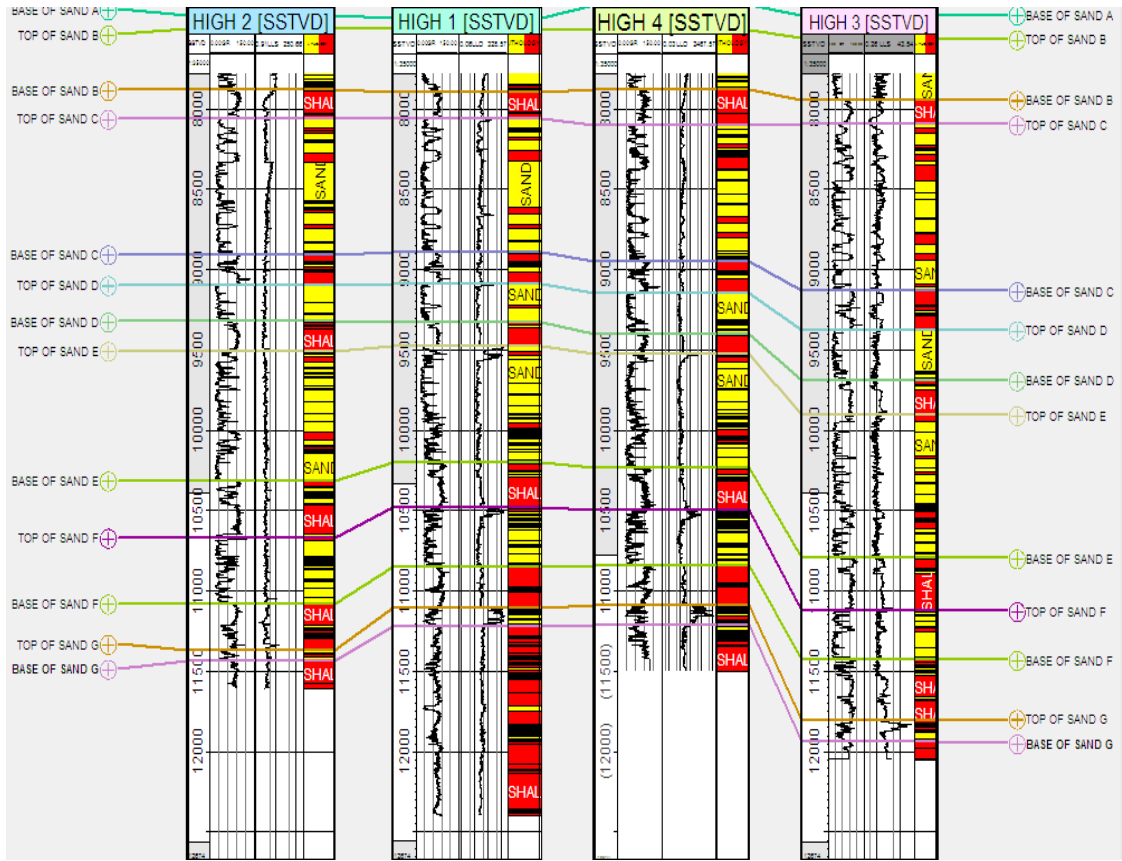


Figure 4b: Lithostratigraphic Well Correlation of Sand C to Sand G along West-East direction

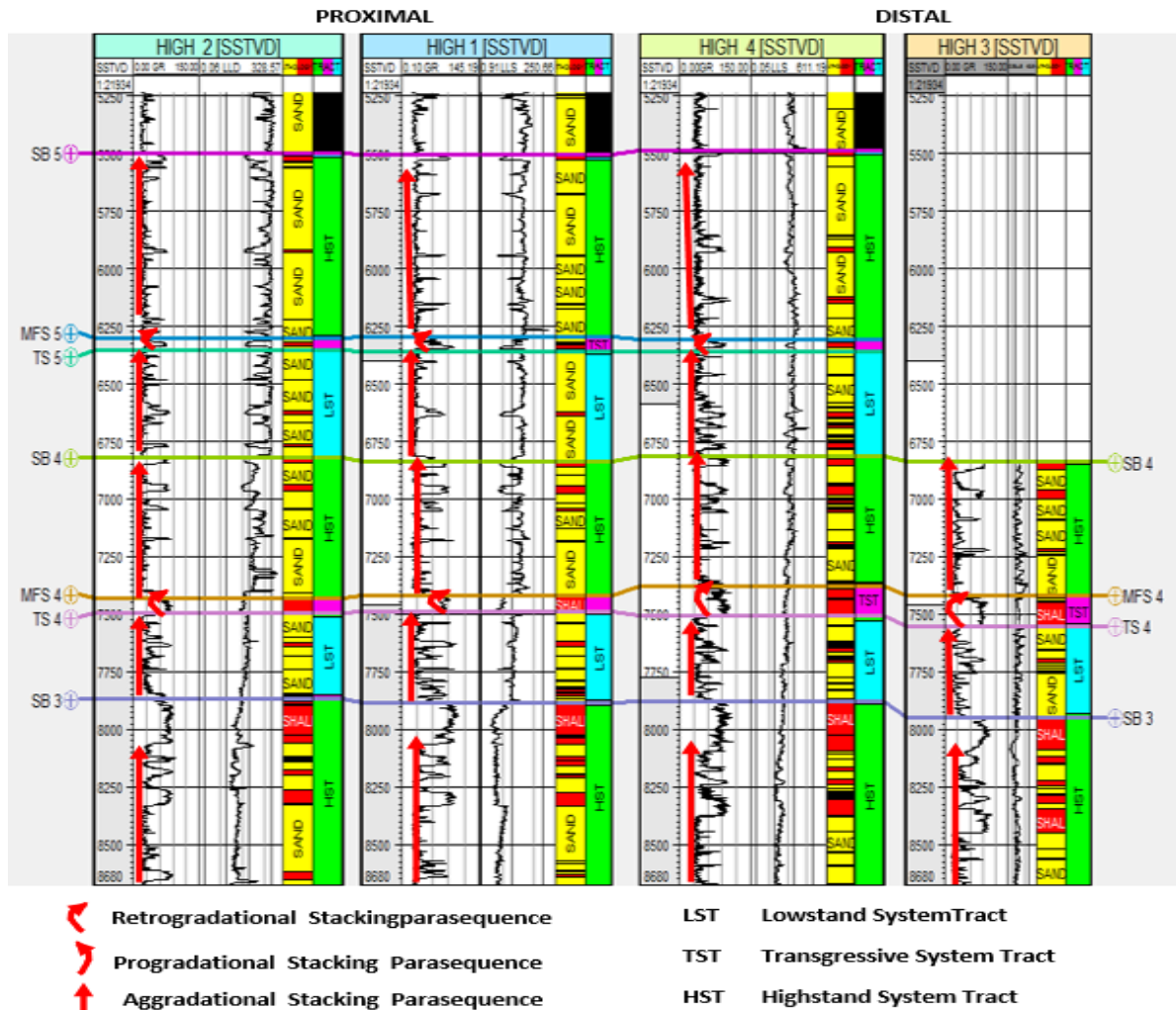
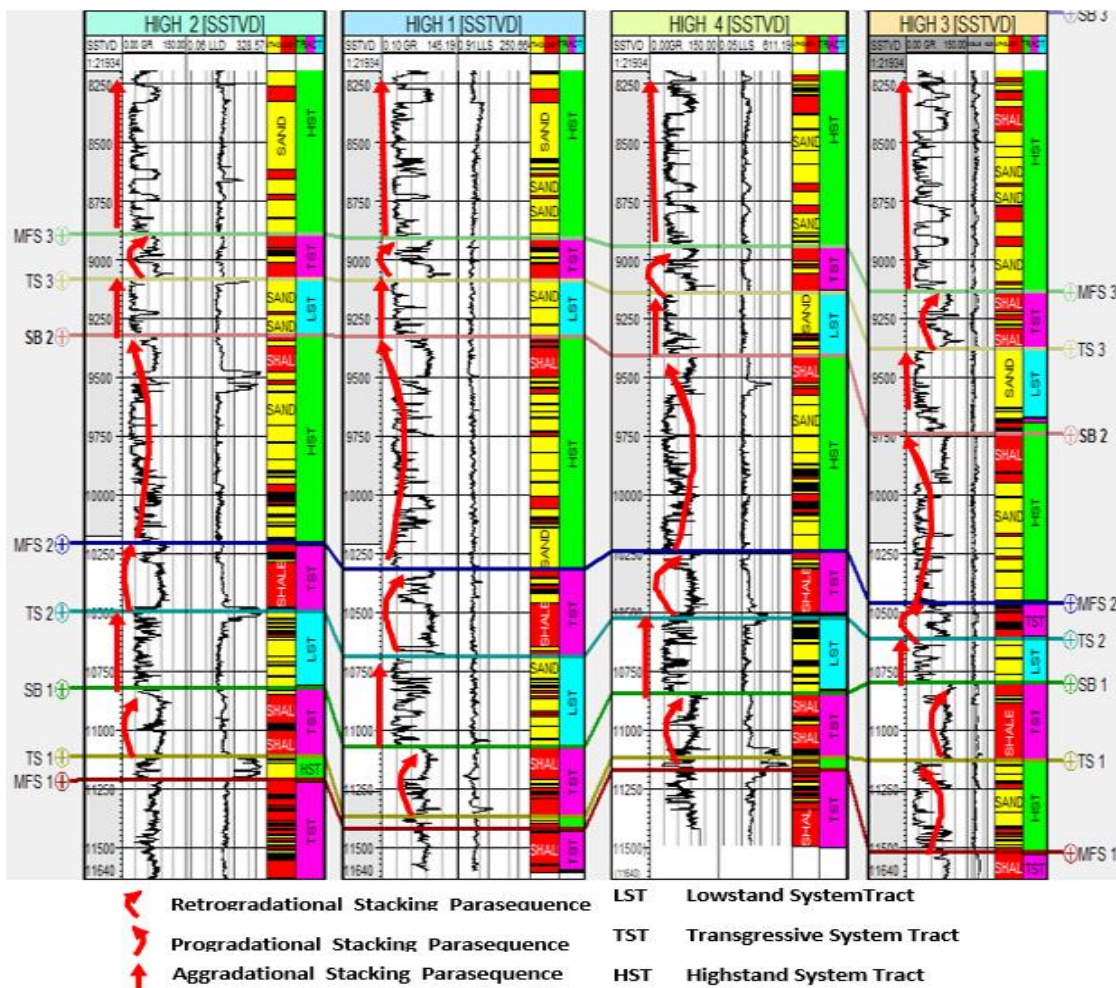
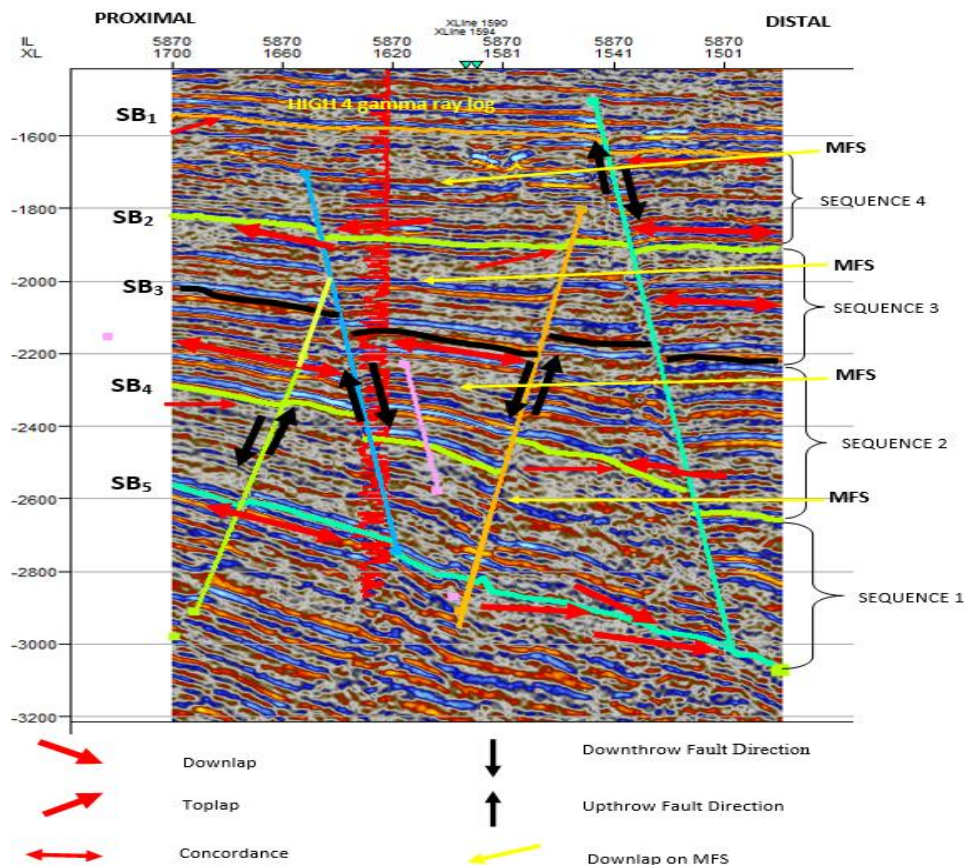


Figure 5a: Identification of Transgressive Surfaces (TS), Maximum Flooding Surfaces (MFS), Sequence Boundaries (SB), and System Tracts (LST, TST, HST).





**Figure 5b:** Identification of Transgressive Surfaces (TS), Maximum Flooding Surfaces (MFS), Sequence Boundaries (SB), and System Tracts (LST, TST, HST) (continued).



**Figure 6:** Interpreted seismic section showing Downlaps, Toplaps, and Concordance Reflection Configurations, Sequence Boundaries SB<sub>1</sub>, SB<sub>2</sub>, SB<sub>3</sub>, SB<sub>4</sub>, and SB<sub>5</sub> on Inline 5870.



3.2.5 Seismic Facies Analysis

Based on seismic reflection frequency and amplitude continuity, three inter-layered seismic facies make up the 3-D seismic volume. Facies I is made up of reflection characteristics that are observed from the seismic record between 0 and approximately 1.35 seconds in terms of two-way travel time. It displays low amplitude, parallel, and discontinuous reflection patterns throughout the field (Figure 7). From gamma ray log, it is uniformly blocky with low value gamma-ray. Since the aim of seismic facies analysis is to infer lithofacies and Environment of Deposition, hence, geologically it is interpreted as consisting of similar lithologies of sand/silty shale that is deposited in either a coastal plain or shallow marine environment with rapid energy changes belonging to the Benin Formation.

Facies II has parallel and high amplitude reflections with a two-way travel

time between 1.35 and 2.8 seconds. It is uniformly blocky with low and high gamma-ray values on the gamma-ray log. The uniform reflectors with moderately high amplitudes that are parallel to sub-parallel show that the majority of sedimentation occurs at a uniform rate. Geologically it is interpreted as consisting of shallow marine deposits of the fluvio-deltaic environment consisting of alternating sand/shale deposits belonging to the Agbada Formation (Figure 7).

Facies III, which are located below the two-way travel time of 2.8 seconds, have a chaotic reflection pattern with low amplitude and frequency discontinuous and discordant reflections. Worthy of note is that the gamma ray log did not penetrate this layer. It is interpreted as the Overpressured marine shale with few streaks of sands (possibly of turbidite origin) that is deposited in a deep water environment belonging to the Akata Formation (Figure 7).

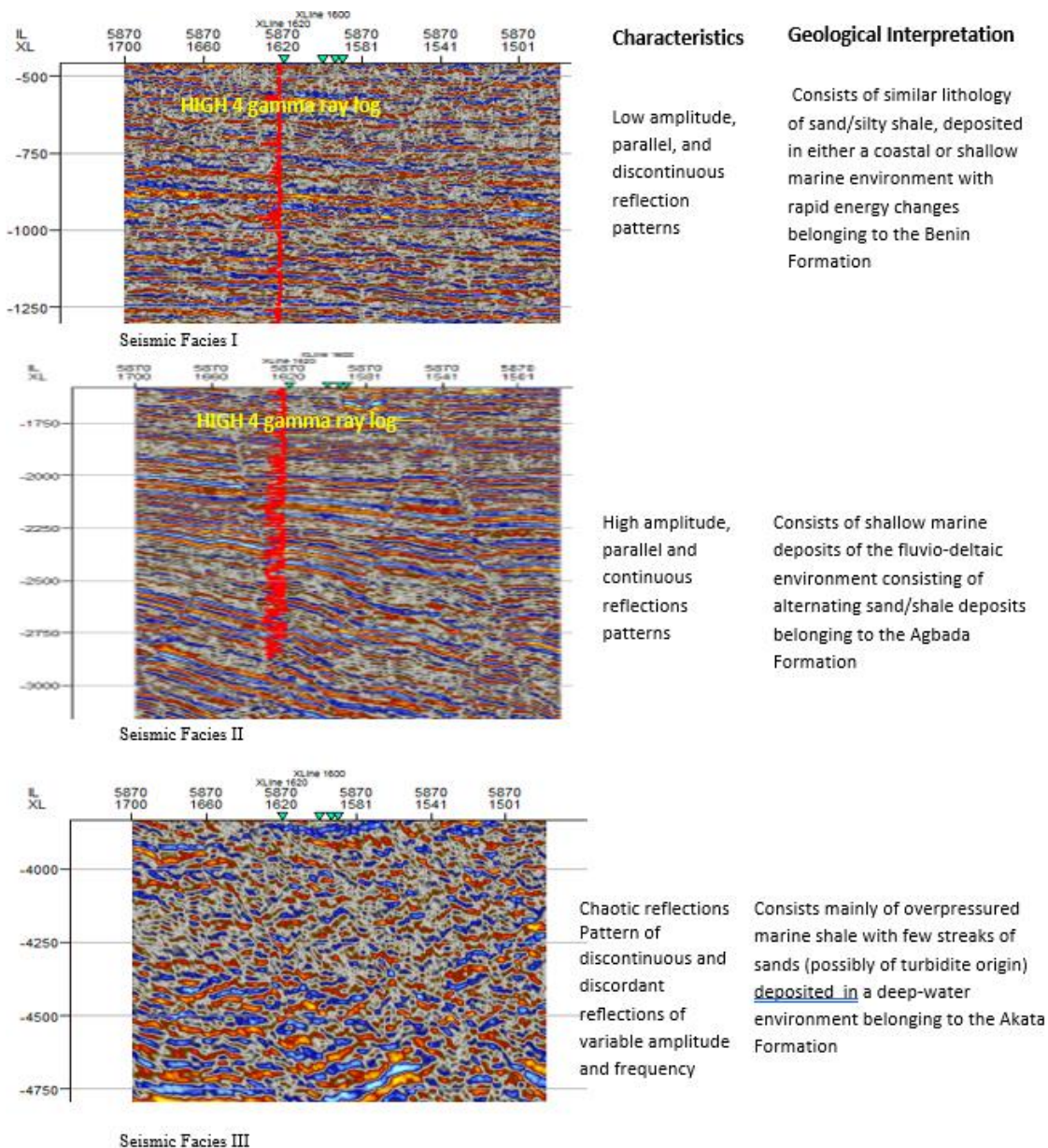


Figure 7: Seismic facies identified within the study area, their characteristics and geological interpretation (gamma ray in red colour on seismic section)

3.2.6 Facies Lateral Distribution using RMS Amplitude Attribute Analysis

The facies lateral distribution using RMS amplitude attributes is shown in Figure 8 to Figure 12. RMS amplitudes, which highlight the variation in acoustic impedance over a chosen sample interval, are a direct indicator of lithology, as was previously mentioned in the previous chapter. While lower RMS amplitude values, shown by light blue/purple color bands, are a clear indication of shale, higher RMS amplitude values, indicated by red, green, or yellow color bands, indicate stacks of sand accumulation but may not necessarily reflect reservoir quality.

RMS Amplitude Attribute For SB<sub>1</sub>

The RMS amplitude attribute map for topmost layer, SB<sub>1</sub> is shown in Figure 8. The map indicates that sand units are concentrated in the southern region and that shale units are dispersed throughout the northeastern and northwest regions. The two primary errors F<sub>1</sub> Seismic Facies III and F<sub>2</sub> is seen to have compact menlised the horizon into three, with abundance of sand decreasing upward from south to north. Higher RMS value, occur at the south-eastern region and may serve as a good prospect P<sub>1</sub> as it is structurally controlled. in the study area.

RMS Amplitude Attribute For SB<sub>2</sub>

Shale units are abundant across a wide lateral extent in Figure 9, while sand units are scarcer and mostly located in the upper right corner, or the



far northeastern area of the map. These shale units can serve as source to the overlying reservoir in SB<sub>1</sub> via the faults especially F<sub>1</sub> since it is laterally extensive.

RMS Amplitude Attribute For SB<sub>3</sub>

Only a few patches of shale units can be seen in the northeast and southwest regions of the map, illustrating the amazing result of the abundance of sand units on SB<sub>3</sub>, as seen in Figure 10. Given that the northern region is structurally high and the area's faults can act as migratory pathways and traps, there is a chance that hydrocarbons will be well-entrapped in the anticlinal structure.

RMS Amplitude Attribute For SB<sub>4</sub>

The RMS amplitude attribute map for SB<sub>4</sub> is displayed in Figure 11. This map demonstrates that there are fewer sand units than shale units because the few sand deposits are only visible in small areas in the northwestern and northeastern regions of the map. While the shale

deposits are widely spread and probably serving as the source and seal of hydrocarbon to the surrounding reservoirs and the major fault F<sub>1</sub> acting as a migratory path way and trap. Interestingly, higher RMS amplitude is seen at north-eastern region of the map and may serve as another good prospect P<sub>2</sub> in the study area as it is also structurally controlled.

RMS Amplitude Attribute For SB<sub>5</sub>

Figure 12 shows the RMS amplitude attribute map for SB<sub>5</sub>. From the map sand units are centrally located and this is further supported by the location of HIGH 1, HIGH 4 and HIGH 3 wells. Moreso, the sand bodies appear as strong reflection events in seismic section. The north-eastern and south-eastern regions of the map show patches of shale units, while the north-eastern and south-eastern regions show patches of sand units.

F<sub>2</sub> is seen to have compactmenlised the horizon into three, with abundance of sand decreasing upward from south to north. Higher RMS value, occur at the south-eastern region and may serve as a good prospect P<sub>1</sub> as it is structurally controlled. in the study area.

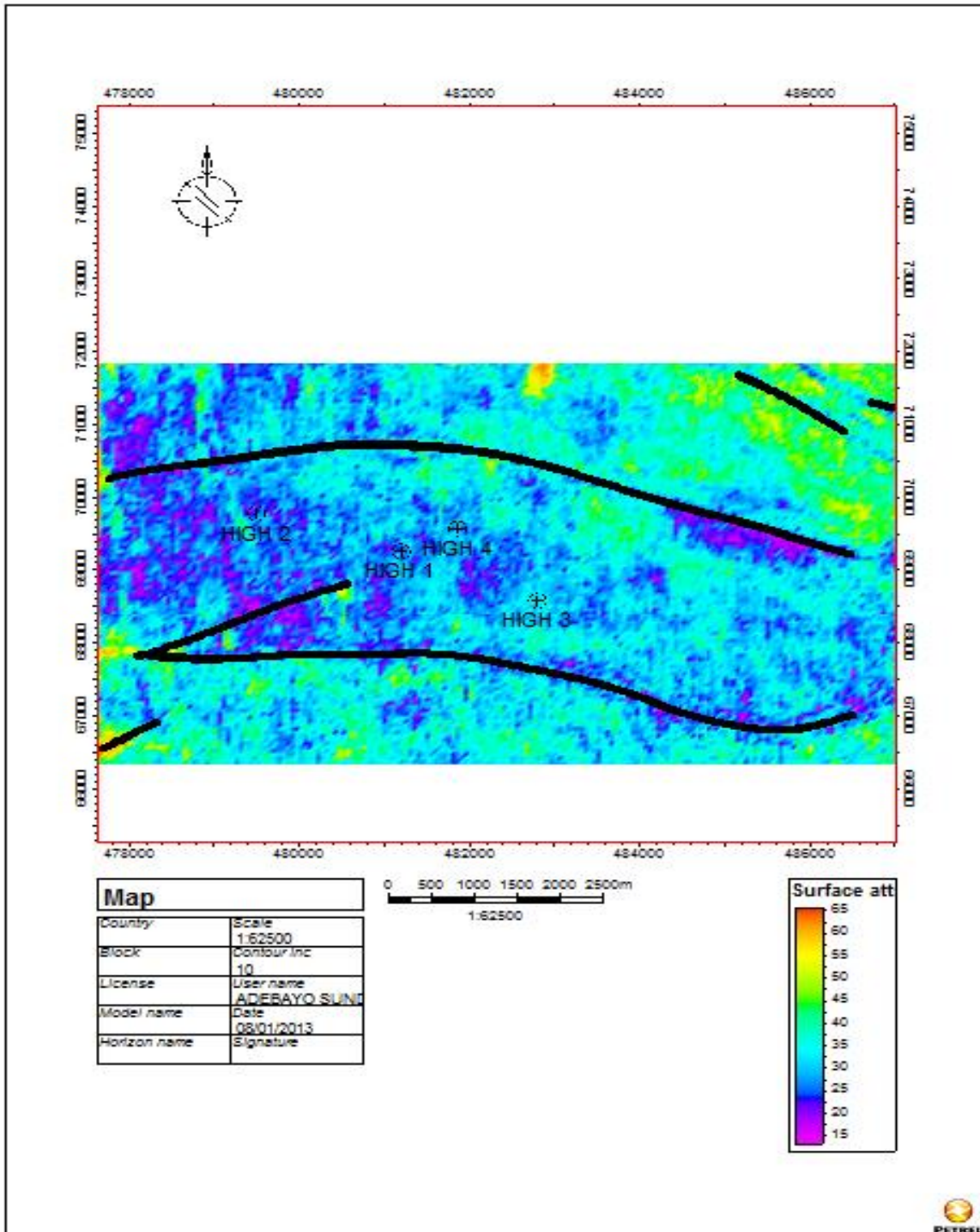


Figure 9: Facies Lateral Distribution Map using RMS Amplitude Attribute For SB<sub>2</sub>

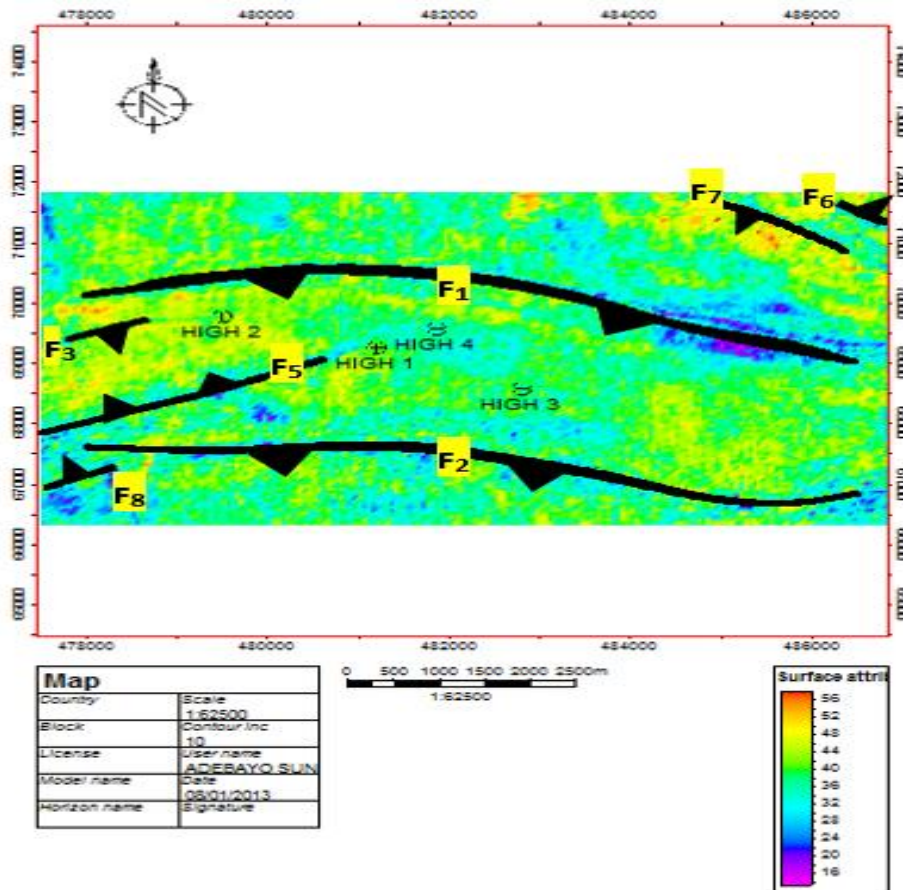


Figure 10: Facies Lateral Distribution Map using RMS Amplitude Attribute For SB<sub>3</sub>

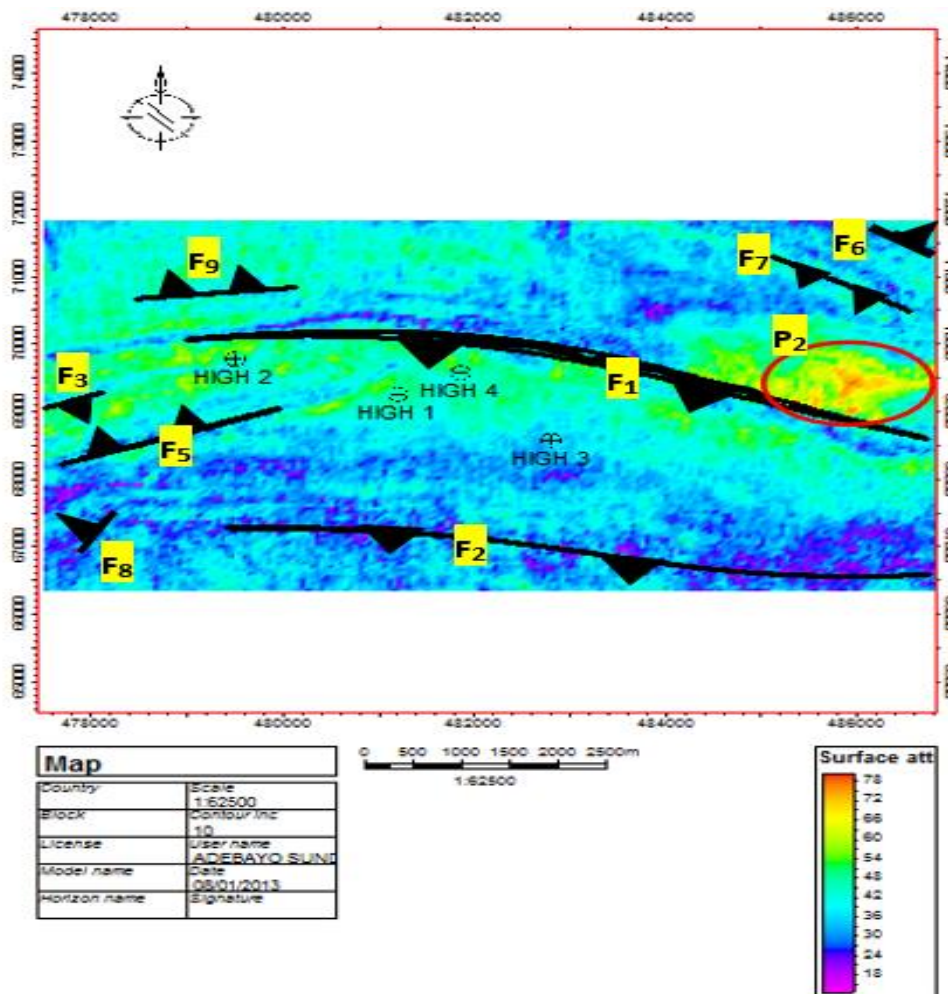


Figure 11: Facies Lateral Distribution Map using RMS Amplitude Attribute For SB<sub>4</sub>

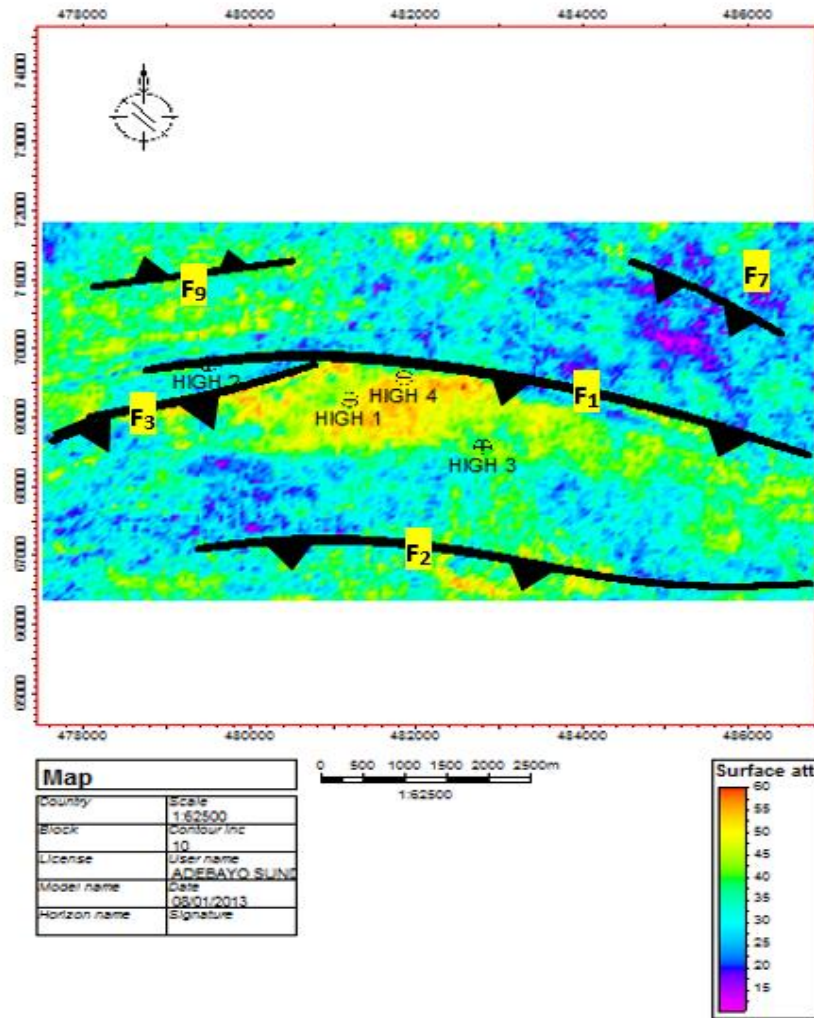


Figure 12: Facies Lateral Distribution Map using RMS Amplitude Attribute For SB<sub>5</sub>

Figure 13 gives a 3-D view of the lateral distribution of the facies in layers from SB<sub>1</sub> to SB<sub>5</sub>. From this figure it is obvious that the wells were drilled to target the sand bodies, particularly on SB<sub>1</sub> and SB<sub>3</sub> where sand bodies are laterally extensive. The lateral distribution of sand and shale units can be seen to be alternating across the five Sequence Boundaries and shows a

decrease in the sand to shale ratio from SB<sub>5</sub> to SB<sub>1</sub> which is a reflection of the Agbada Formation characteristics. Vertical distribution of these identified facies can best be done using geostatistical tools which is beyond the scope of this work.

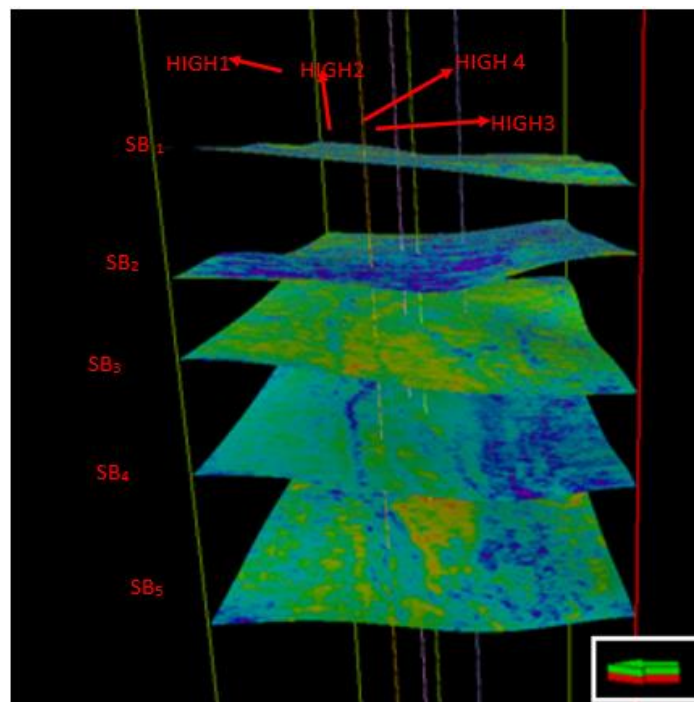


Figure 13: 3-D View of Facies distribution and wells showing that the wells drilled to target the sand bodies particularly on SB<sub>1</sub> and SB<sub>3</sub>.



3.2.7 Interpretation of Environments of Deposition

In light of the lack of biostratigraphic and core data, the depositional environments were inferred from all of the wells using a combination of resistivity curve signatures and gamma ray signatures, as illustrated in Figure 14a-l. The log pattern can be symmetrical, irregular, bell-shaped, funnel-shaped, or cylindrical.

According to standard interpretations of the Agbada Formation (Weber 1971; Orife and Avbovbo 1982; Owoyemi and Willis 2006), prograding delta deposits are thought to be represented by log successions that progressively decrease in gamma-ray value and then rapidly increase (gradually coarsen and then abruptly fine, i.e. symmetrical trend). This was recognized in HIGH 2 at depth intervals 11752-11700 ft (3582-3566 m) and 11224-11099 ft (3421-3383 m) among others, in HIGH 1 at depth interval 10469-10400 ft (3191-3170 m) and 10400-10347 ft (3170-3154 m) among others, in HIGH 4 at depth intervals 11162-11084 ft (3402-3367 m) among others, and in HIGH 3 at depth intervals 11877-11800 ft (3620-3597 m) and 10900-10847 ft (3322-3306 m) among others.

Relics of fining and coarsening upward small scale, monolithic, high energy, fast deposit of very coarse sand known as channel sands can be seen in a cylindrical or blocky log pattern. These sands are limited to the proximal fluvio-marine environment, with an abrupt base that represents the erosional base of the channel fill sequence. This was recognized in HIGH 2 at the depth intervals 9856 - 9532 ft (3004-2905 m) and 9222-9083 ft (2811-2769 m) among others, in HIGH 1 at depth intervals 9300-9092 ft (2835-2771 m) and 9722-9571 ft (2963-2917 m) among others, in HIGH 4, at the depth intervals 9915-9570 ft (3022-2917 m) and 10229 - 10082 ft (3139-3073 m) among others, in HIGH 3 at the depth intervals 10449-9947 ft (3200-3032 m) and 9670-9375 ft (2947-2858 m) among others.

It can be deduced from this study therefore that the cylindrical depositional motif is significant of distributary channel sand deposited within a shallow marine environment.

Both prograding delta and channel deposits (sands) constitute excellent hydrocarbon reservoirs. They are always found at the centre between two maximum flooding surfaces. The maximum flooding surfaces act as regional seal rocks while other flooding surfaces may just be locally sealing within the field.

The funnel-shaped log pattern represents barrier sand, also known as beach sand, which is coarsening upward with the river mouth deposit of the distributary channel and increasing upward in energy of deposition as the coastline moves toward the sea over geologic time. Regressive behaviors are what define it. At HIGH 2, this was recognized at the depth intervals 9526-9474 ft (2903-2888 m) and 9565-9500 ft (2915-2896 m) for HIGH 1, 9571-9527 ft (2917-2904 m) for HIGH 4 and 9942-9900 ft (3030-3018 m) for HIGH 3 among other occurrences in the wells.

The shoreline environment is where barrier bar sand is most prevalent, and the lithofacies that are related to it are offshore silts with interbedded hemipelagic shales and shoreface sands. According to Coleman and Prior's (1980) analysis, the gamma ray log's irregular shape, also known as the serrated high gamma ray, indicates that the log facies is part of a basin plain environment. The environment has low lithologic variation and high lateral continuity, characterized by a blanket of fine silts and clays deposited from suspension. As illustrated in Figure 14 a-l, they are identified on every well and have a light blue color.

As geologic time passes and the coastline shifts landward, the bell-shaped log pattern is narrowing upward due to a decrease in deposition energy. Sand that has been altered and reworked to resemble meandering channels is most commonly found along shorelines and other shallow marine environments. It is distinguished by actions that are transgressive. In HIGH 2, this was identified at the depth intervals 9954-9900 ft (3034-3018 m), and in HIGH 1 at depth interval 10000-9951 ft (3048-3033 m), 8948-8900 ft (2727-2713 m) for HIGH 4 and 8349-8300 ft (2544-2530 m) for HIGH 3.

3.2.8 Depositional Energy and Lithofacies Identification

In this study, the depositional energy trend—which is helpful in identifying sedimentary facies follows two sequences (Posamentier and Vail, 1988). They are the ones with upward sequences that are coarsening and fining. Individuals with upward fining sequences are slender. With the coarser grains indicating a lower energy of deposition and the finer grains indicating a higher energy of deposition, this constitutes the lithologic classification showing the building up of sandstone from coarse to fine grains. The deposits are thicker in the coarsening upward sequences, which decrease in thickness from sandstone at the top to shale at the base (Figure 14a-l).

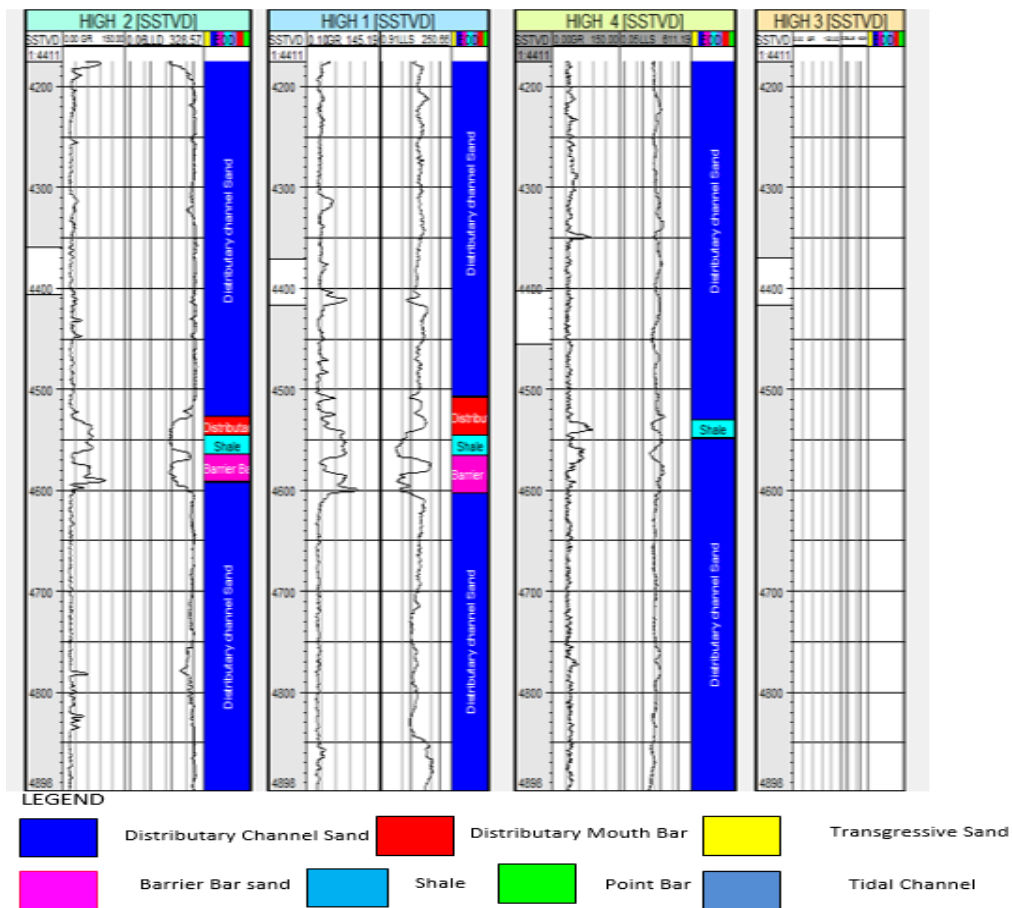


Figure 14a: Identifying Environments of Deposition (EOD) Using Log Motif.

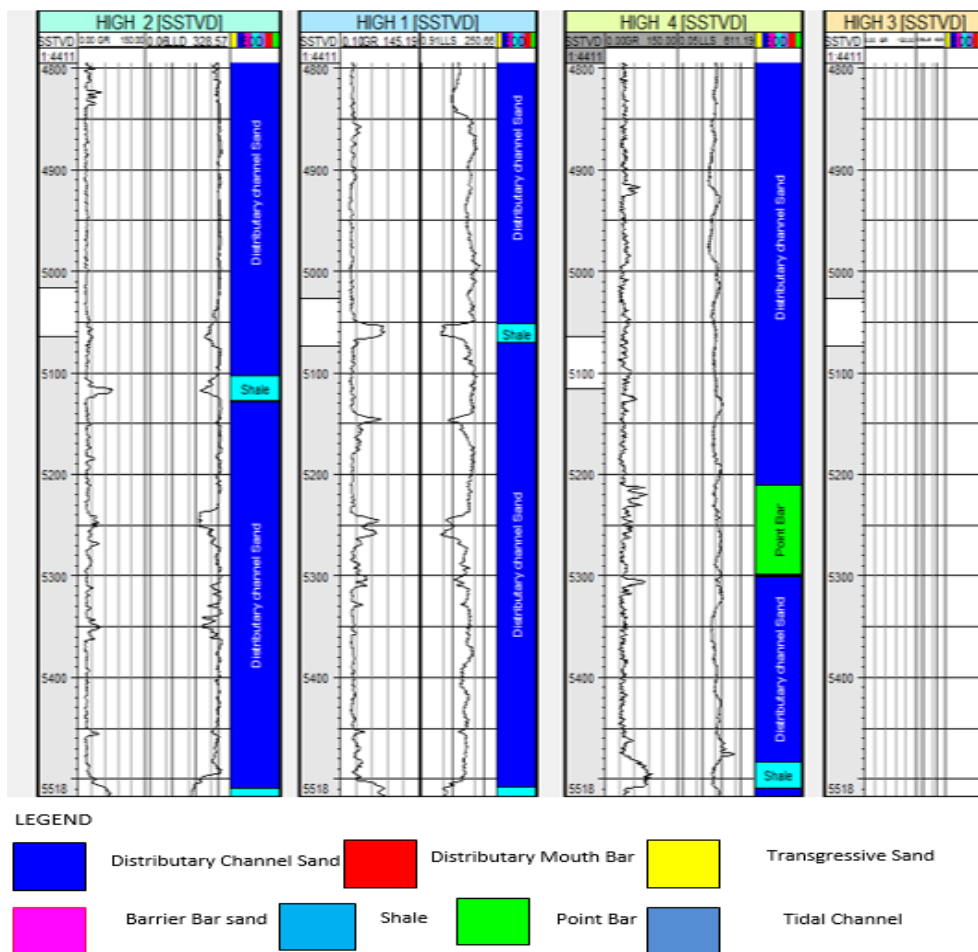


Figure 14b: Identifying Environments of Deposition (EOD) Using Log Motif (continued)

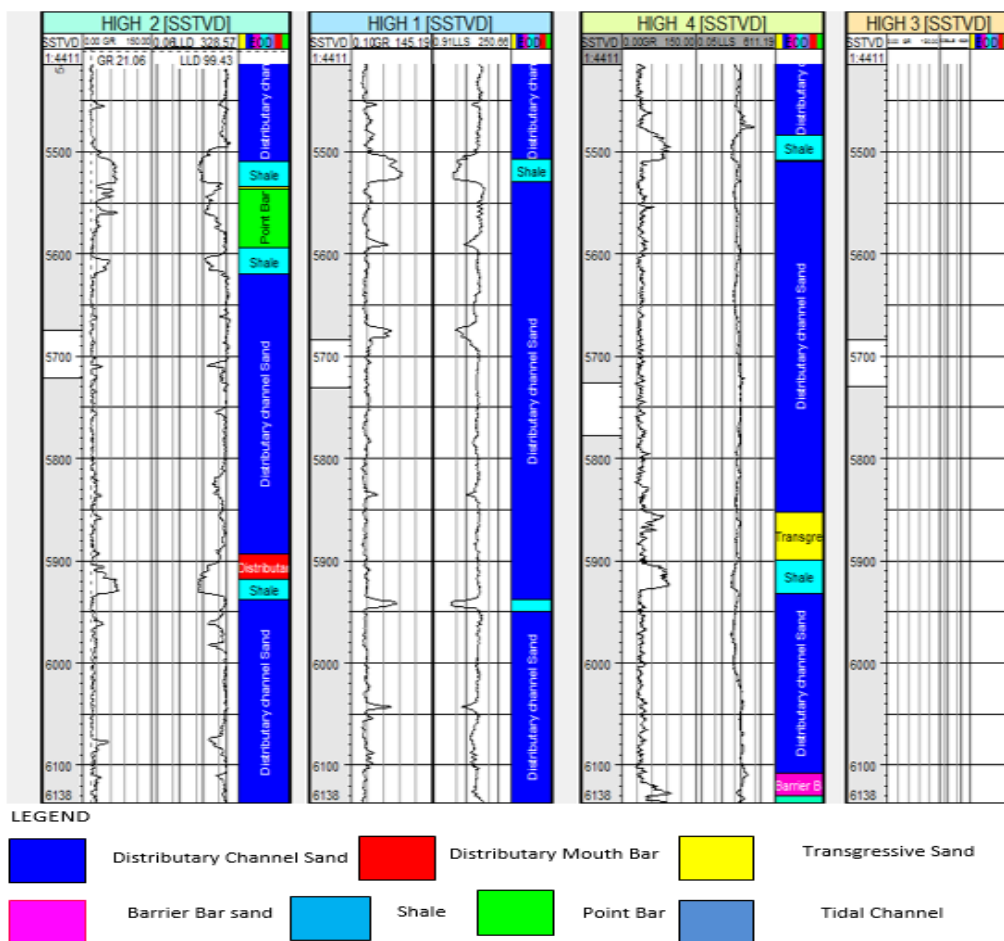


Figure 14c: Identifying Environments of Deposition (EOD) Using Log Motif (continued)

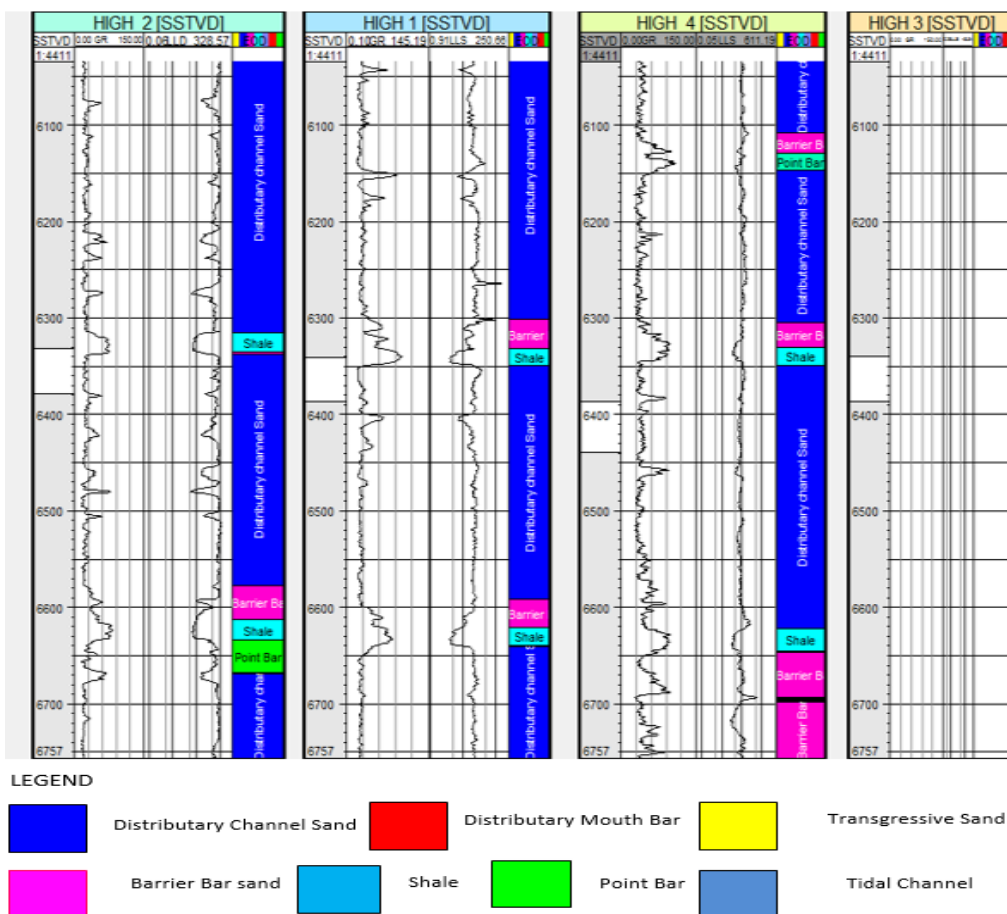


Figure 14d: Identifying Environments of Deposition (EOD) Using Log Motif (continued).

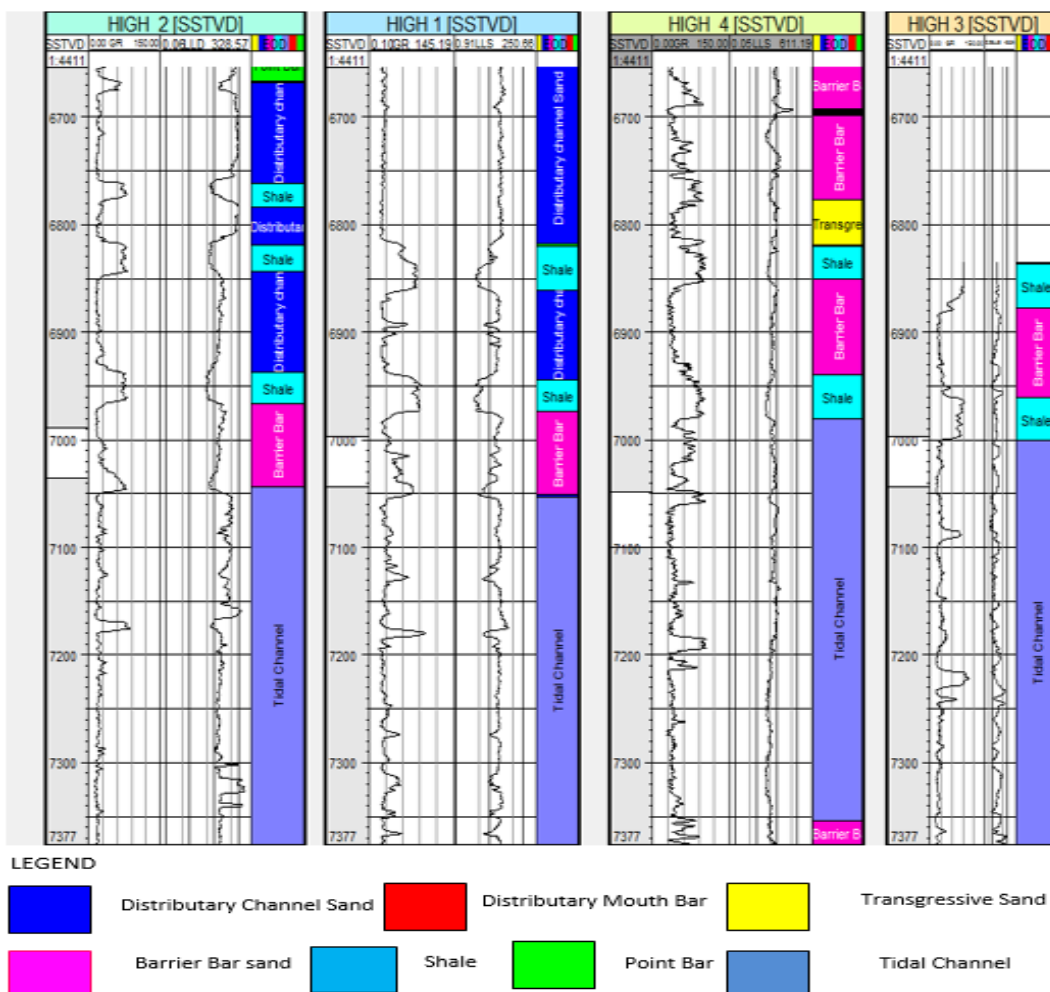


Figure 14e: Identifying Environments of Deposition (EOD) Using Log Motif (continued).



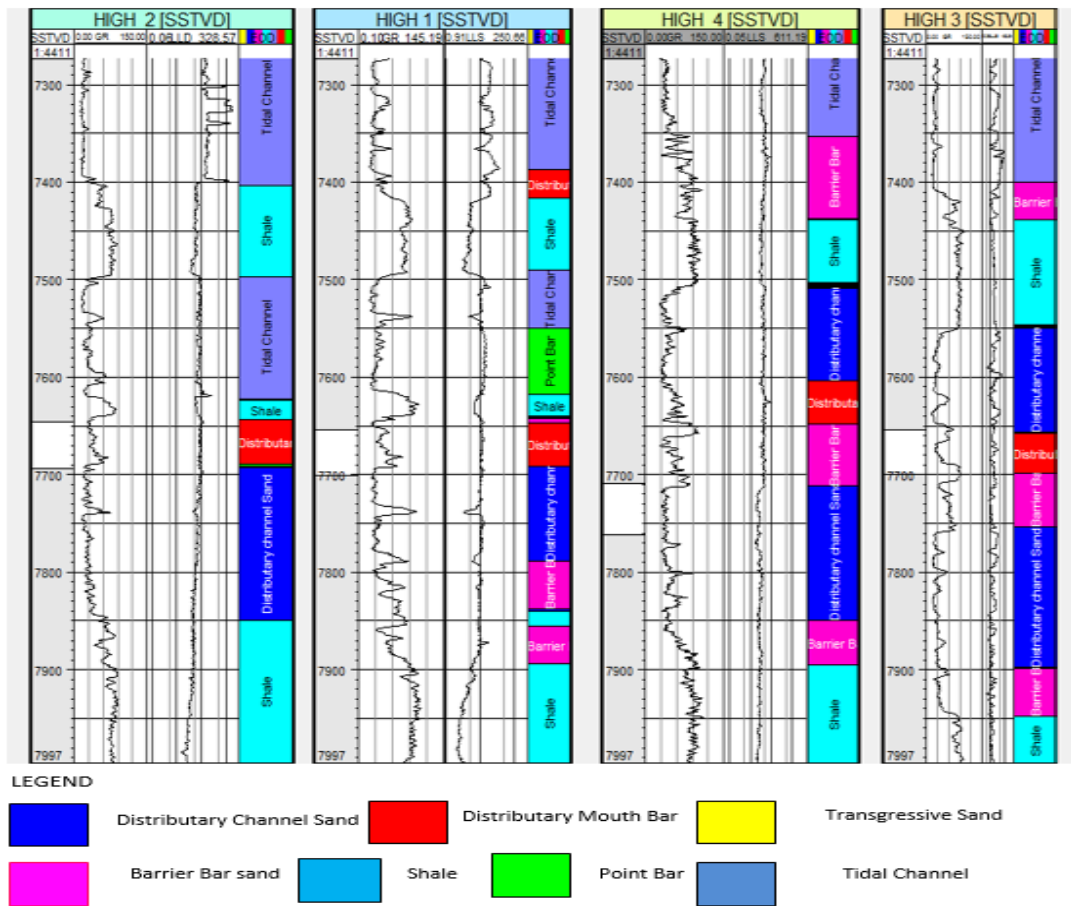


Figure 14f: Identifying Environments of Deposition (EOD) Using Log Motif (continued).

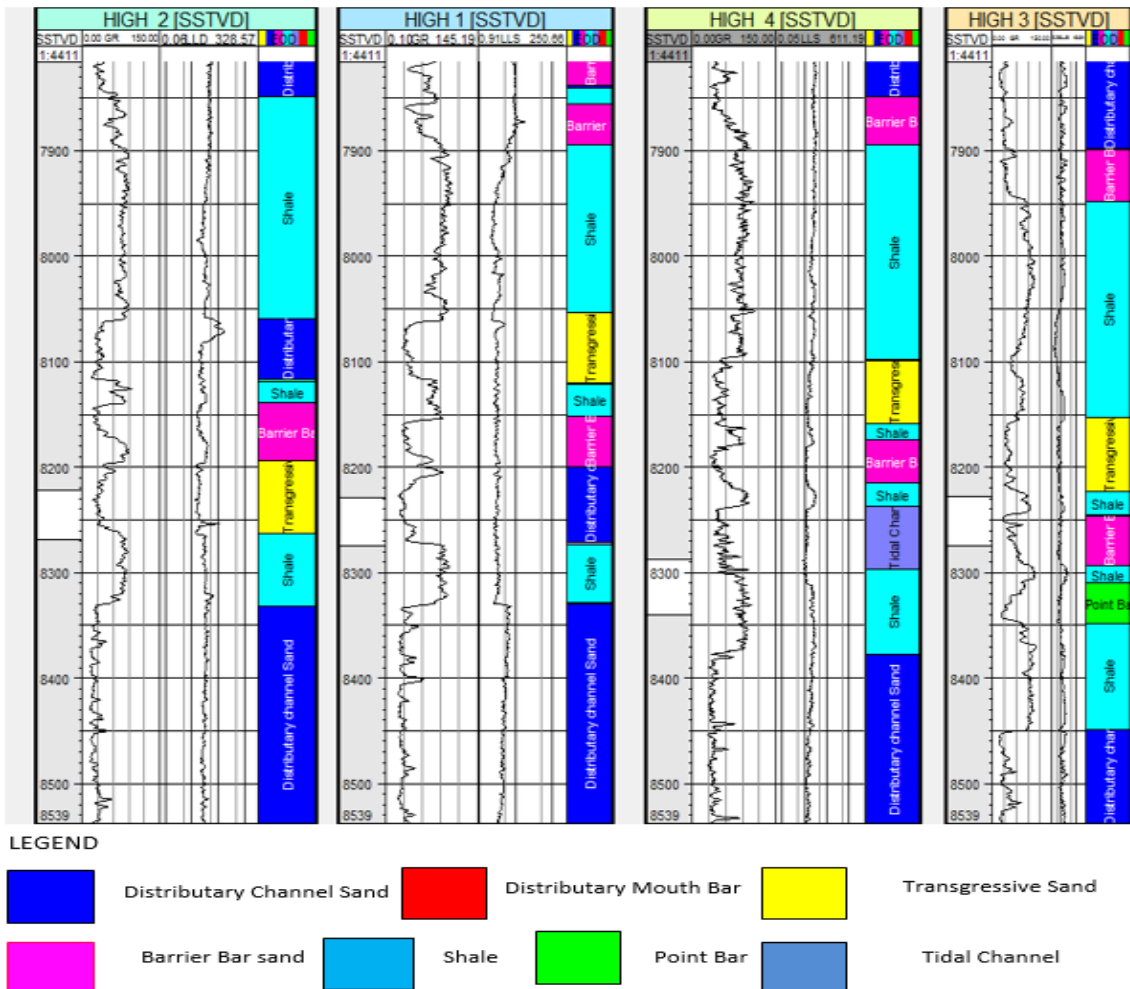


Figure 14g: Identifying Environments of Deposition (EOD) Using Log Motif (continued).

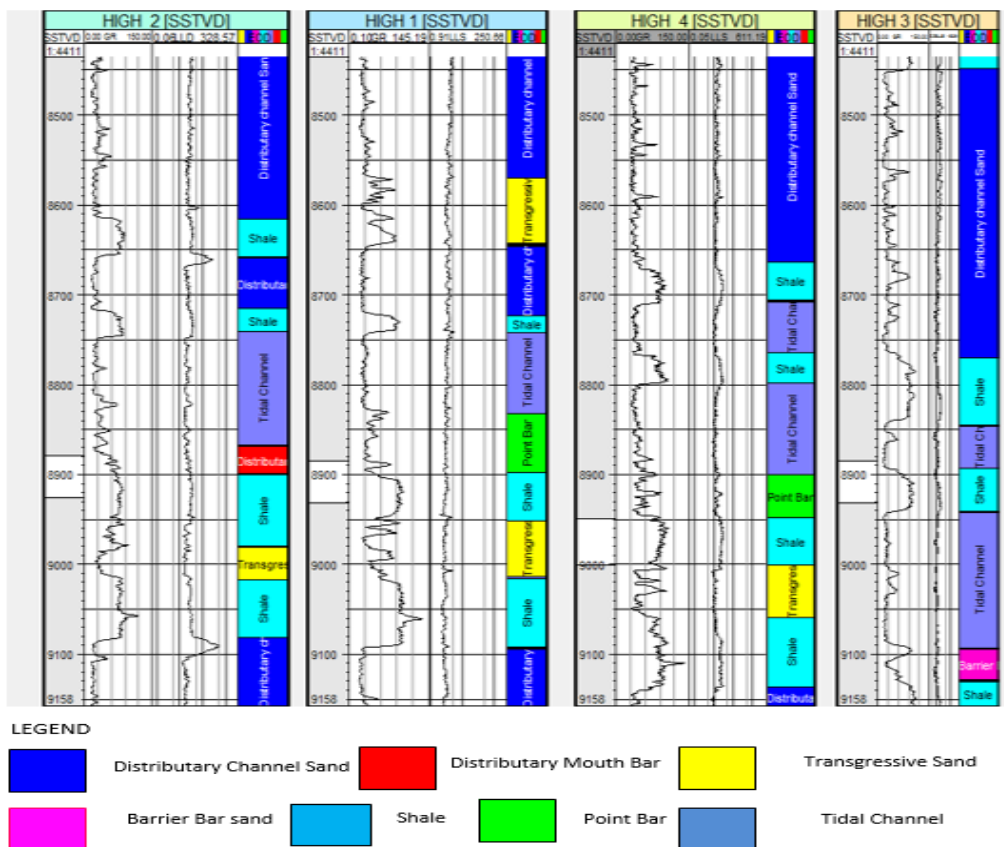


Figure 14h: Identifying Environments of Deposition (EOD) Using Log Motif (continued).

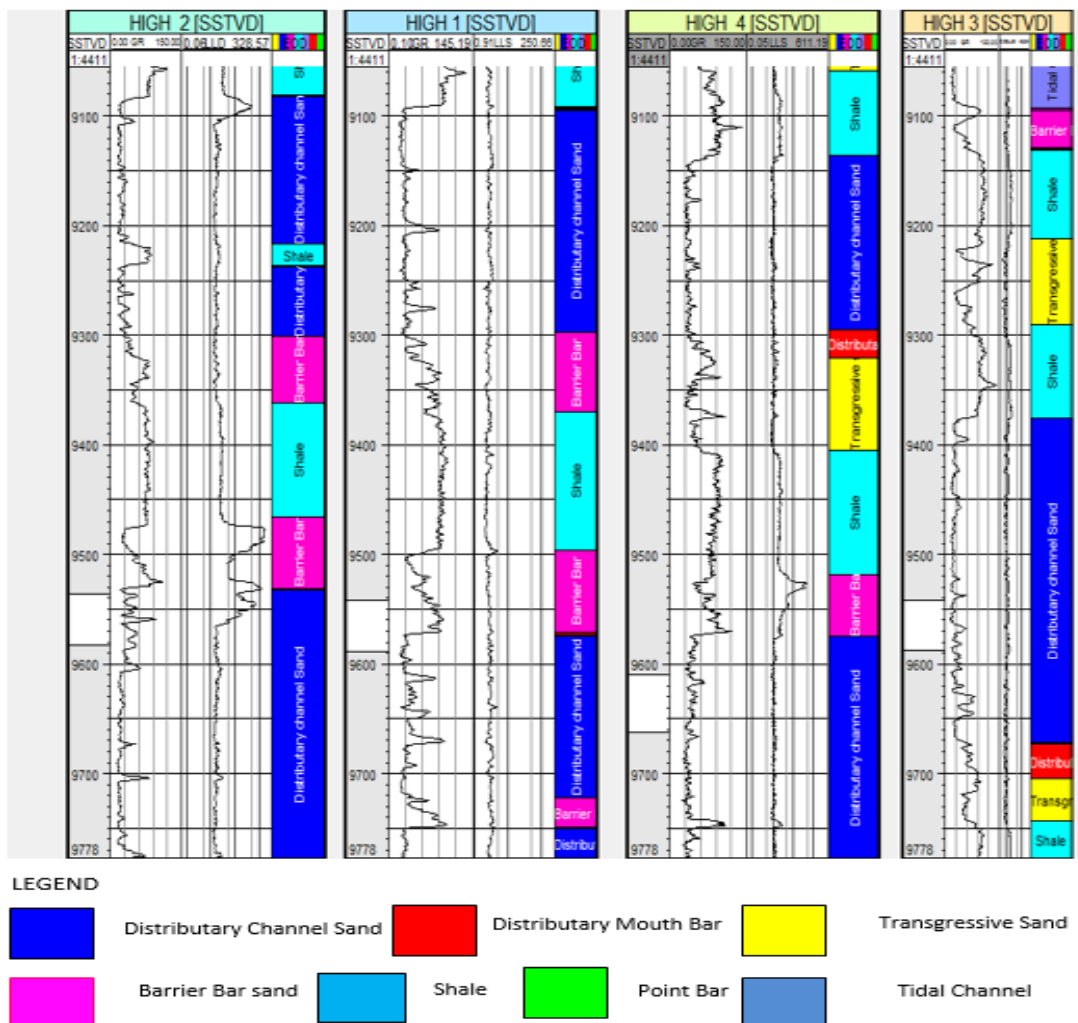


Figure 14i: Identifying Environments of Deposition (EOD) Using Log Motif (continued).

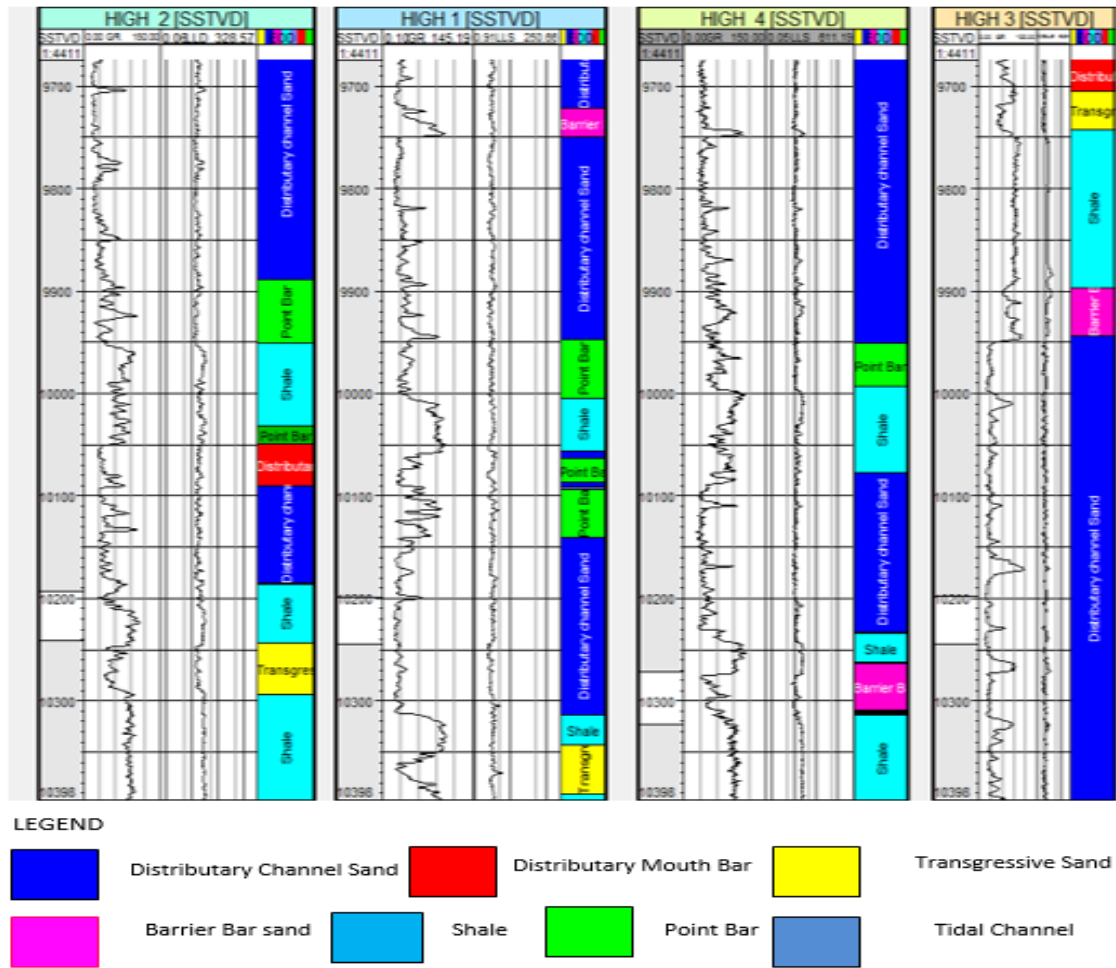


Figure 14j: Identifying Environments of Deposition (EOD) Using Log Motif (continued).

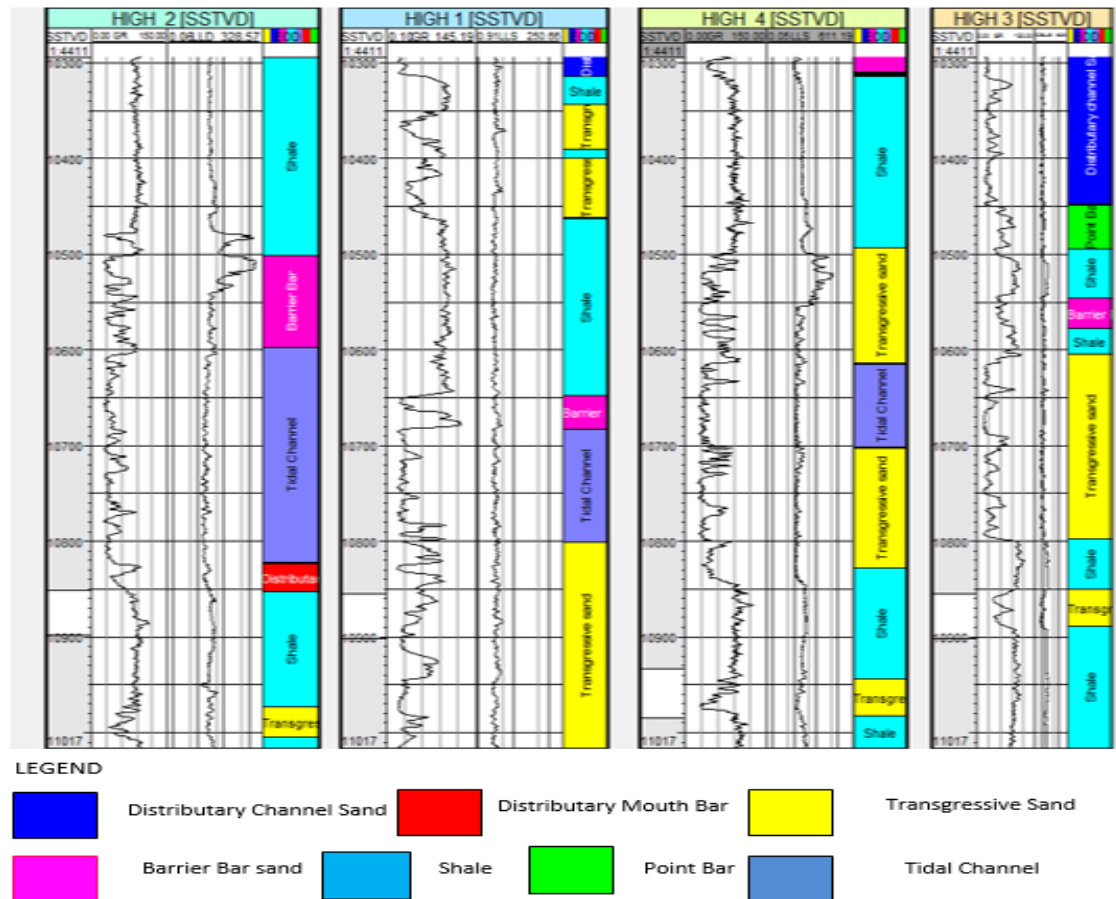


Figure 14k: Identifying Environments of Deposition (EOD) Using Log Motif (continued).



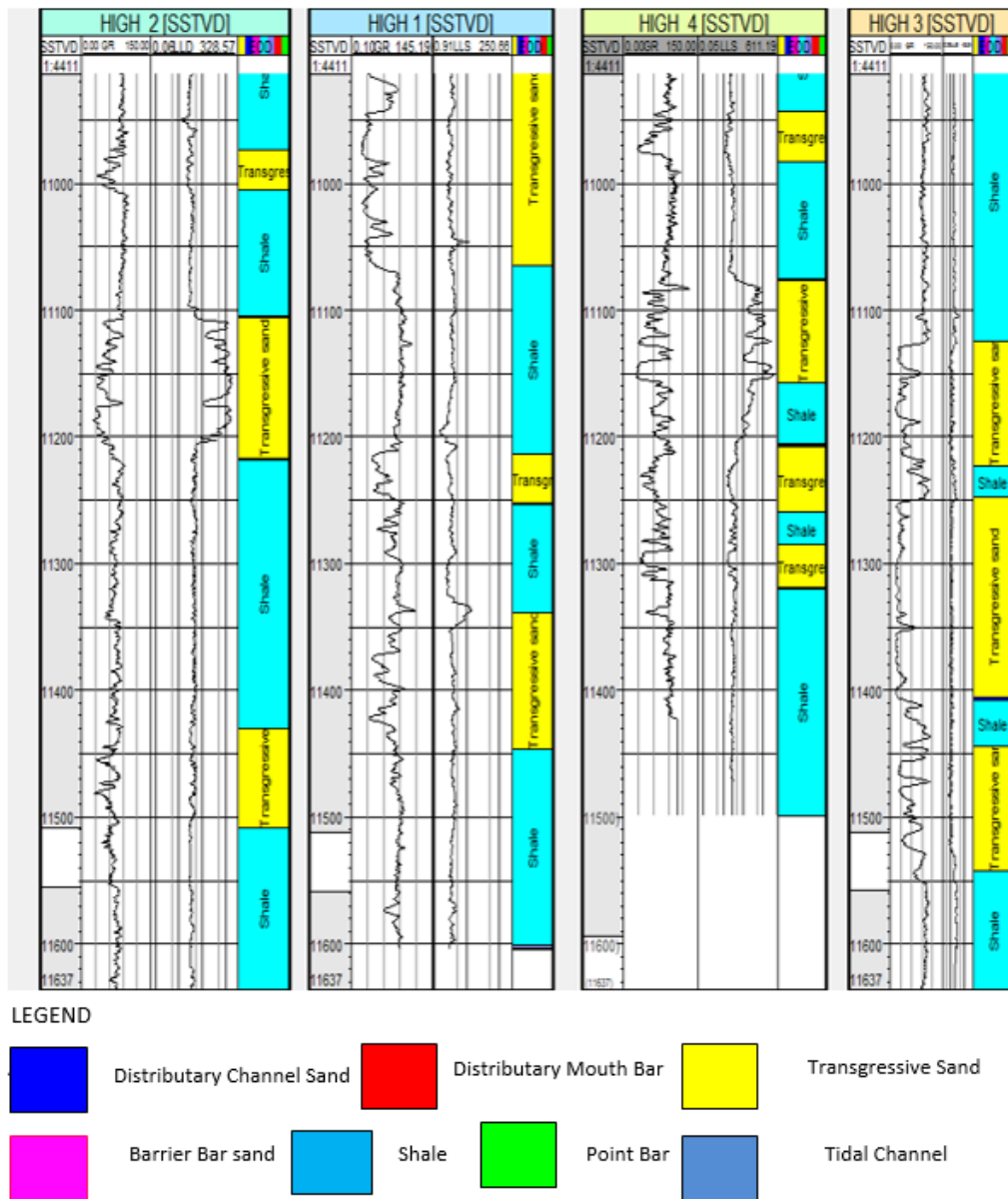


Figure 14I: Identifying Environments of Deposition (EOD) Using Log Motif (continued).

4. CONCLUSION AND RECOMMENDATION

Sequence boundaries, maximum flooding surfaces, and transgressive surfaces were identified by sequence stratigraphic analysis as important bounding surfaces and subtle stratigraphic traps that are caused by the rapid facies changes that take place between successive systems tracts. A favorable environment for the generation and accumulation of organic matter is suggested by the cyclical pattern of the alternating LST, TST, and HST in the study region. Under the correct circumstances, the pelagic shales of the transgressive systems tract could serve as suitable source and cap rocks for the underlying LST and overlying HST, respectively. Sands with reservoir quality found in the LST and HST may make suitable reservoirs. From the facies distribution map analysis two (2) new prospects P<sub>1</sub> (485098,66860.78) and P<sub>2</sub> (485898.74,69538.67) were identified which can be further analysed for profitable hydrocarbon exploitation and may increase the reserves together with the existing producing reservoirs of HIGH1(481200.00, 69280.00), HIGH2 (479500.00,69800.00), HIGH3 (482800.00,68600.00) and HIGH4 (481860.00,69595.00) wells.

RECOMMENDATION

Comprehensive Well Log-Seismic Sequence stratigraphic interpretation combines seismic reflection profiles, high resolution biostratigraphic, and paleobathymetric data with well logs. Hence, it is recommended that well log data and 3-D seismic profiles should be augmented with core and biostratigraphic data for a proper interpretation of depositional environment and the checkshot data for other wells should be made available for a more reliable depth conversion process.

REFERENCES

Adejebi AR, Olayinka AI, 1997. Stratigraphy and hydrocarbon potential of the Opuama channel complex area, western Niger delta. Nigerian Association of Petroleum Exploration (NAPE) Bulletin., 12: 110.

Aizebeokhai AP, Olayinka I, 2011. Structural and stratigraphic mapping of Emi field, offshore Niger Delta. Journal of Geology and Mining Research Vol. 3(2), pp. 25-38.

Allen JRL, 1965. Late Quaternary Niger Delta, and adjacent areas—sedimentary environments and lithofacies: American Association of Petroleum Geologists Bulletin, volume 49, pp.547-600.

Avbovbo AA, 1978. Tertiary lithostratigraphy of Niger Delta: American Association of Petroleum Geologists Bulletin, volume. 62, p. 295-300.

Ayuk MA, Akinyemi OD, Mohammed MZ, 2022. Integrating rock physics and sequence stratigraphy for characterization of deep-offshore turbidite sand system. Journal of African Earth Sciences, Vol.193.

Barde JP, Chambertain P, Gralla P, Harwijanto J, Marsky J, Schroeter T, 2000. Explaining a complex hydrocarbon system in the Permo-Triassic of the precaspian basin by integration of independent models. Abstracts, 62nd European Association of Geoscientists and Engineers Conference and Technical Exhibition, 2: (P.021), p. 4

Barde JP, Gralla P, Harwijanto J, Marsky J, 2002. Exploration at the eastern edge of the precaspian basin impact of data integration on Upper Permian and Triassic prospectivity. American Association Petroleum

- Geology Bulletin., 86: 399-415.
- Beka FT, Oti MN, 1995. The distal offshore Niger Delta: frontier prospects of a mature petroleum province, in, Oti, M.N., and Postma, G., eds., *Geology of Deltas*: Rotterdam, A.A. Balkema, p. 237-241.
- Burke K, 1972. Longshore drift, submarine canyons and submarine fans in development of Niger Delta, American Association of Petroleum Geologists Bulletin volume. 56:1975-1983.
- Cobos LS, 2005. Structural Interpretation of the Monagas Foreland Thrust Belt, Eastern Venezuela. Adapted from extended abstract prepared for presentation at American Association of Petroleum Geologists Annual Convention, Dallas, Texas, April 17-21, 2004.
- Coffen JA. 1984. Interpreting seismic data: Penwell Publishing Company, Tulsa Oklahoma. pp. 39-118.
- Doust H, Omatsola E, 1989. Niger Delta, in, Edwards, J. D., and Santogrossi, P.A., eds., *Divergent/passive Margin Basins*, American Association of Petroleum Geologists Memoir 48: Tulsa, American Association of Petroleum Geologists, p. 239-248.
- Emery D, Myers K. 1996. *Sequence Stratigraphy*. Blackwell Science Ltd., London, UK. 297.
- Evamy BD, Haremboure J, Kamerling P, Knaap WA, Molloy FA, Rowlands PH, 1978. Hydrocarbon habitat of Tertiary Niger Delta, American Association of Petroleum Bulletin volume. 62, p. 277-298.
- Hooper RJ, Fitzsimmons RJ; Grant N, Vendeville BC. 2002. The role of deformation in controlling depositional patterns in the South-Central Niger Delta, West Africa: *Journal of Structural Geology*, volume. 24, p. 847-859.
- Ileebare1 M, Omorogieva OM. 2020. Formation Evaluation of the Petrophysical Properties of wells in e - field Onshore Niger Delta, Nigeria. *Nigerian Journal of Technology (NIJOTECH)*. Vol. 39, No. 4, October 2020, pp. 962 – 971
- Jervey MT, 1988. Quantitative geological modeling of siliciclastic rock sequences and their seismic expression In: Wilgus, C. K., Hastings, B. S., Kendall, C. G. St. C., Posamentier, H. W., Ross, C. A., Van Wagoner, J. C.(eds.), *Sea Level Changes – An Integrated Approach*. Society of Economic Paleontologists and Mineralogists (SEPM) Special Publication 42, 47–69
- Kendall CST, Moore P, Strobel JS, Cannon RL, Perlmutter M, Bezdek J, Biswas G. 1991. Simulation of the Sedimentary Fill of Basins: in Franseen, E. K., Watney, W. L., Kendall, C. G. St. C., Ross, W., eds., *Sedimentary Modeling: Computer Simulations and Methods for Improved Parameter Definition*, Kansas Geological Survey Bull. 233, p. 9–30.
- Mitchum RM, Sangree JB, Vail PR, Wornardt WW, 1993. Recognizing sequences and systems tracts from well logs, seismic data, and biostratigraphy: Examples from the late Cenozoic of the Gulf of Mexico, in P. Weimer and H. Posamentier ,eds., *Siliciclastic sequence stratigraphy: Recent developments and applications*: American Association of Petroleum Geologists Memoir 58, p. 163–197.
- Mitchum RM, Van Wagoner JC, 1990. High-frequency sequences and eustatic cycles in the Gulf of Mexico Basin. [In:] J.M. Armentrout & B.F. Perkins (Eds): *Sequence stratigraphy as an exploration tool-concepts and practices in the Gulf Coast*. Gulf Coast rSection, SEPM, Program and Abstracts Eleventh Annual Research Conference, Houston, p. 257–267.
- Nwachukwu JI, Chukwurah PI, 1986. Organic matter of Agbada Formation, Niger Delta, Nigeria: American Association of Petroleum Geologists Bulletin, v. 70, p. 48-55.
- Nwangwu U, 1990. A unique, hydrocarbon trapping mechanism in the offshore Niger Delta, in Oti, M.N., and G. Postma, eds., *Geology of Deltas*: Rotterdam, A. A. Balkema, p.269-278.
- Oomkens E. 1974. Lithofacies relations in late Quaternary Niger delta complex: *Sedimentology*, v.21, p.195-222.
- Orife JM, Avbovbo AA, 1982. Stratigraphic and unconformity traps in the Niger Delta: American Association of Petroleum Geologists, Bulletin, Vol. 65, pp.251–265.
- Owoyemi AO, Willis BJ. 2006. Depositional patterns across syndepositional normal faults, Niger Delta, Nigeria: *Journal of Sedimentary Research*, Vol. 76, pp.346–363.
- Owoyemi AOD, 2004. The sequence Stratigraphy of Niger Delta, Delta field, offshore Nigeria. Unpublished M. Sc. Thesis, Texas A&M University, 88 p.
- Posamentier HW, Jervey MT, Vail PR. 1988. Eustatic controls on deposition I-conceptual framework; in, sea level changes- An Integrated Approach, Wilgus, C.K;Hastings, B.S., Kendall, C. G. St.C., Posamentier, H.W., Ross, C. A., and Van Wagoner J. C., eds.: *Society of Economic Paleontologists and Mineralogists, Special Publication 42*, p.109-124
- Posamentier HW, Vail PR. 1988. Eustatic controls on clastic deposition II – Sequence and systems tracts models, in C.K., Wilgus, B.S. Hastings, C.G. St. C.
- Sangree JB, Vail PR, Mitchum Jr RM, 1990. A summary of exploration applications of sequence stratigraphy, in J. M. Armentrout and B. F. Perkins, eds., *Sequence stratigraphy as an exploration tool— Concepts and practices in the Gulf Coast (abs.)*: Gulf Coast Section SEPM 11th Annual Research Conference, Houston, Texas, Program and Abstracts, p. 321–327
- Short KC, Stauble AJ. 1967. Outline of Geology of Niger Delta: American Association of Petroleum Geologists Bulletin volume 51, p. 761-779.
- Stacher P, 1995. Present understanding of the Niger Delta hydrocarbon habitat, in, Oti, M.N., and Postma, G., eds., *Geology of Deltas*: Rotterdam, A.A. Balkema, p. 257-267.
- Stacher P, Ozumba BM, Ehoche, P., 1993. Revised Chronostratigraphic and Sequence Stratigraphic Chart, Niger Delta, Nigeria, S.P.D.C. Exploration Report no 93-01.
- Tuttle MLW, Charpentier RR, Brownfield ME. 1999. The Niger delta petroleum system: Niger delta province, Nigeria, Cameroon, and Equatorial Guinea, Africa: USGS Open-file report 99-50-H.
- Umar A, Hucai Z, Aqsa A, Muhammad A, Xiaonan Z, Saiq SA, Hassan NM. 2020. Controls on Reservoir Heterogeneity of a Shallow-Marine Reservoir in Sawan Gas Field, SE Pakistan: Implications for Reservoir Quality Prediction Using Acoustic Impedance Inversion. *Water* 2020, 12, 2972; doi:10.3390/w12112972
- Weber KJ, 1971. Sedimentological aspects of oil fields in the Niger Delta. *Geologie en Mijnbouw*50, 559–576.
- Whiteman AJ. 1982. Nigeria: Its Petroleum Geology: Resources and Potential.1 and 2. Graham and Trotton: London, UK. 394.

